*Electronic Research Archive*

https://www.aimspress.com/journal/era

ERA, 33(12): 7918–7956.
DOI: 10.3934/era.2025349
Received: 26 October 2025
Revised: 07 December 2025
Accepted: 16 December 2025
Published: 25 December 2025

*Research article*

# Bifurcation analysis in a diffusive predator-prey model with distributed memory and gestation delay

**Doudou Lou, Yunxian Dai* and Weidong Qin**

Department of Mathematics, Kunming University of Science and Technology, Kunming, Yunnan 650500, China

* **Correspondence:** Email: dyxian@kust.edu.cn.

**Abstract:** This paper proposes and studies a predator-prey model incorporating distributed memory and gestation delay to more accurately describe animal movement. First, the stability conditions of the positive equilibrium in the absence of delays are analyzed. Second, the conditions for the occurrence of Turing and Hopf bifurcation without gestation delay are derived. Subsequently, the combined effects of memory delay and gestation delay on the stability of the positive equilibrium are investigated, revealing that their interaction can generate more complex spatiotemporal patterns. Furthermore, normal form theory is employed to determine the direction and stability of the Hopf bifurcation induced solely by memory delay in the absence of gestation delay. Finally, numerical simulations are conducted to validate the theoretical results. In addition, variations in the memory-based diffusion coefficient, memory delay, and gestation delay are shown to trigger transitions among spatially homogeneous/nonhomogeneous steady states and spatially homogeneous/nonhomogeneous periodic patterns.

**Keywords:** spatial memory; distributed delay; gestation delay; Hopf bifurcation; normal form

## 1. Introduction

The study of predator-prey dynamics occupies a central role in mathematical ecology. While predators depend on prey for survival, excessive predation can drive prey populations to extinction, ultimately leading to the collapse of the predator population, as well. Unlike direct predation, which reduces prey numbers through mortality, fear effects as evidenced by numerous studies [1–5] can exert broader and longer-lasting influences on prey populations by altering their behavior, life-history traits, and spatial distribution within ecosystems. Biologists have observed that lots of biological phenomena can induce the Allee effect, such as antipredator defence among the prey, mating difficulty, and environmental conditions. A population needs to maintain a minimum density in order

to avoid extinction, and this minimum density is referred to as an Allee threshold [6–10]. Considering these biological elements, Harine et al. [11] put forward a predator-prey model with (i) a fear effect in a prey population, (ii) an Allee effect in a predator population, and (iii) a variable attack rate which adjusts the functional response:

$$\begin{cases} \frac{dx}{dt} = \frac{rx}{1+ky} - r_0 x - r_1 x^2 - \frac{ax^2 y}{bx^2+x+c}, \\ \frac{dy}{dt} = \frac{\eta a x^2 y}{bx^2+x+c}\left(\frac{y}{y+\theta}\right) - my, \end{cases} \tag{1.1}$$

where $x, y$ are the density of prey and predator; $r$, $r_0$, and $r_1$ denote the birth rate, the death rate, and the intraspecific competition; $\frac{1}{1+ky}$ is the fear level function, where $k$ denotes the cost of fear in prey; $\frac{ax^2y}{bx^2+x+c}$ is the variable attack rate functional response, where $a$ denotes the maximally achievable attack rate and $c$ denotes the half saturation constant, and the prey population at which the attack rate is $a/2$, $b$ denotes the product of a maximally achievable attack rate and handling time; $\eta$ denotes the conversion coefficient of prey biomass to predator biomass; $\frac{y}{y+\theta}$ is the Allee function, where $\theta$ denotes the strength of the Allee effect; and $m$ denotes the death rate of predator. The authors ensured the non-negativity and boundedness of the solutions and examined the local and global stability of each equilibrium.

Animals possess memory and cognitive abilities that significantly shape their movement behavior [12–15]. To avoid predation, prey species often use past experience to relocate to areas historically associated with lower predator density; predators likewise rely on memory of prey distribution over time to improve hunting efficiency [16, 17]. By incorporating spatial memory into models, numerous scholars have investigated its impact on animal movement patterns and the underlying mechanisms [18–22]. Shi et al. [19] proposed a single-species model with discrete memory delay to describe the influence of memory on the animal movement. Song et al. [20] developed a consumer-resource model incorporating a discrete delay to investigate the effect of consumers' memory on the spatial distribution of resources. The authors focused on discrete memory delays in their research [19, 20]. Because memory fades over time, information regarding past locations becomes increasingly difficult to retrieve later. Biologically, gradient-tracking movement based on distributed memory (i.e., memory spanning past time periods) is more realistic than that relying on memory at a specific past time point. Building on this insight, Shen et al. [21] incorporated a distributed memory delay into the memory-driven diffusion term to examine the impact of such a distributed delay on the dynamics of the diffusive resource-consumer model.

In recent years, a number of models incorporating dual delays have been proposed. For instance, Li [23] developed a spatial model with memory delay in prey, Allee effect, and maturation delay with delay-dependent coefficients for predators, aiming to understand species' spatial distribution. Wang [24] focused on analyzing the spatiotemporal dynamics of the model to reveal how spatial memory and reproductive cycles influence the spatiotemporal distribution of prey. Nevertheless, to the best of our knowledge, very few studies to date have examined systems with two delays in which one of them is a distributed delay. Thus, on the basis of the model proposed in [11], we further establish a diffusion model with the spatial memory through spatiotemporal distributed delay and the gestation delay $\sigma$, where the population density $u(x,t), v(x,t)$ satisfies

$$\begin{cases} \frac{\partial u(x,t)}{\partial t} = d_{11}\Delta u(x,t) + \frac{ru(x,t)}{1+kv(x,t)} - r_0 u(x,t) - r_1 u^2(x,t) - \frac{au^2(x,t)v(x,t)}{bu^2(x,t)+u(x,t)+c}, & 0 < x < l\pi, t > 0, \\ \frac{\partial v(x,t)}{\partial t} = d_{22}\Delta v(x,t) - d_{21}\left[v(x,t)w_x(x,t)\right]_x - mv(x,t) + \frac{\eta a u^2(x,t-\sigma)v(x,t-\sigma)}{bu^2(x,t-\sigma)+u(x,t-\sigma)+c}\left(\frac{v(x,t)}{v(x,t)+\theta}\right), & 0 < x < l\pi, t > 0, \\ u_x(x,t) = v_x(x,t) = 0, & x = 0, l\pi, t \geq 0, \\ u(x,t) = u_0(x,t), v(x,t) = v_0(x,t), & 0 < x < l\pi, -\tau \leq t \leq 0, \end{cases} \tag{1.2}$$

where $d_{11}, d_{22} > 0$ denotes the self-diffusion coefficient of populations $u(x,t), v(x,t)$. $d_{21}$ denotes the memory-based diffusion coefficient. For $d_{21} > 0$, predators move from low prey density to high prey density. On the contrary, when $d_{21} < 0$, predators tend to migrate to low prey density areas, and it indicates that there is no memory-driven diffusion when $d_{21} = 0$.

In this work, we utilize the memory-based distribution function presented in [25], which takes the following form:

$$w(x,t) = G * h * u = \int_{-\infty}^{t} \int_{0}^{l\pi} G(x,y,t-\xi)h(t-\xi)u(y,\xi)dyd\xi.$$

Here, the spatiotemporal kernel function $G(x,y,t)$: $(0,l\pi)\times(0,l\pi)\times[0,+\infty) \to \mathbb{R}^+$ denotes

$$G(x,y,t) = \sum_{n=0}^{+\infty} e^{-d_{22}\mu_n t}\phi_n(x)\phi_n(y),$$

satisfying the normalization condition

$$\int_{0}^{l\pi} G(x,y,t)dx = 1, \quad y \in (0,l\pi), \quad t > 0,$$

where $\mu_n$ are the eigenvalues of the negative Laplacian eigenvalue problem, satisfying

$$0 = \mu_0 \le \mu_1 \le \mu_2 \le \cdots \le \mu_j \le \cdots,$$

and $\lim_{j\to+\infty} \mu_j = +\infty$ and $\phi_n(x)$ are the corresponding normalized eigenfunctions of $\mu_n$.

We adopt a weak delay kernel, given by

$$h(t) = \frac{1}{\tau}e^{-t/\tau}, \tau > 0,$$

satisfying the normalization conditions $\int_0^{+\infty} h(t)dt = 1$ and $\int_0^{+\infty} th(t)dt = \tau$. This kernel function exhibits a strictly decreasing trend with respect to the variable $t$, which reflects that the memory of animals can become ambiguous over time.

Nonlinear systems can exhibit rich dynamical behaviors, including Hopf bifurcation, Turing bifurcation, and Turing–Hopf bifurcation, among others. The normal form plays an important role in bifurcation analysis, as it allows one to determine the direction and stability of bifurcating solutions. For reaction-diffusion systems with delay confined to the reaction term, Faria [26] introduced an algorithm for computing the normal form of Hopf bifurcation. More recently, Wu et al. [27] developed computational methods for reaction-diffusion systems incorporating both delay and nonlocal spatial averaging. In [21], Shen et al. first proposed a consumer-resource model with distributed memory and applied normal form theory to determine the direction and stability of the Hopf bifurcation induced by the mean delay. In the present work, we employ the approach established in [21] to derive the normal form of Hopf bifurcation for model (1.2), thereby characterizing its direction and stability.

This paper is structured as follows. In Section 2, we investigate the stability conditions of the positive equilibrium without delays and the conditions for the occurrence of Turing bifurcation and

Hopf bifurcation without the gestation delay. In addition, the joint impact of distributed memory delay and gestation delay on the stability of the positive equilibrium of system (1.2) is investigated along with the induced bifurcation patterns. In Section 3, the normal form theory is used to determine the direction and stability of Hopf bifurcation caused by the distributed memory delay without the gestation delay. The numerical simulations are used to illustrate the theoretical results in Section 4. Finally, Section 5 presents the conclusions and discussion of this work.

## 2. Stability and Hopf bifurcation of system (1.2)

In this section, we first investigate the stability conditions of the positive equilibrium $E_*$ without delays. Then, we provide the conditions for the occurrence of Turing bifurcation and Hopf bifurcation when the gestation delay $\sigma = 0$ and the memory delay $\tau > 0$. Finally, we discuss the stability conditions of the positive equilibrium $E_*$ when $\sigma \geq 0$ and $\tau \geq 0$.

Let $E_* = (u_*, v_*)$ be the positive equilibrium, which satisfies the following equation

$$\begin{cases} \dfrac{ru_*}{1+kv_*} - r_0u_* - r_1u_*^2 - \dfrac{au_*^2v_*}{bu_*^2+u_*+c} = 0, \\ \dfrac{\eta au_*^2v_*}{bu_*^2+u_*+c}\left(\dfrac{v_*}{v_*+\theta}\right) - mv_* = 0. \end{cases} \tag{2.1}$$

Then, the linearized system of system (1.2) at $E_*$ is

$$\begin{pmatrix} u_t \\ v_t \end{pmatrix} = D_1\begin{pmatrix} \Delta u \\ \Delta v \end{pmatrix} + D_2\begin{pmatrix} \Delta w \\ \Delta v \end{pmatrix} + A\begin{pmatrix} u \\ v \end{pmatrix} + B\begin{pmatrix} u_\sigma \\ v_\sigma \end{pmatrix}, \tag{2.2}$$

where

$$D_1 = \begin{pmatrix} d_{11} & 0 \\ 0 & d_{22} \end{pmatrix}, D_2 = \begin{pmatrix} 0 & 0 \\ -d_{21}v_* & 0 \end{pmatrix}, A = \begin{pmatrix} \alpha_{11} & \alpha_{12} \\ 0 & \alpha_1 \end{pmatrix}, B = \begin{pmatrix} 0 & 0 \\ \beta_{21} & \alpha_2 \end{pmatrix}, \tag{2.3}$$

and

$$\alpha_{11} = \frac{r}{1+kv_*} - r_0 - 2r_1u_* - \frac{au_*v_*(u_*+2c)}{(bu_*^2+u_*+c)^2}, \alpha_{12} = -\frac{rku_*}{(1+kv_*)^2} - \frac{au_*^2}{bu_*^2+u_*+c} < 0,$$
$$\alpha_1 = -m + \frac{\eta\theta au_*^2v_*}{(\theta+v_*)^2(bu_*^2+u_*+c)}, \beta_{21} = \frac{\eta au_*v_*^2(u_*+2c)}{(\theta+v_*)(bu_*^2+u_*+c)^2} > 0, \alpha_2 = \frac{\eta au_*^2v_*}{(\theta+v_*)(bu_*^2+u_*+c)}.$$

We assume

$$\begin{pmatrix} u(x,t) \\ v(x,t) \end{pmatrix} = \sum_{n=0}^{\infty}\begin{pmatrix} \alpha_n \\ \beta_n \end{pmatrix} e^{\lambda_n t}\phi_n(x) \tag{2.4}$$

is the solution of linearized system (2.2). Substituting (2.4) into system (2.2), through some simple calculations, we obtain

$$\Delta w(x,t) = -\mu_n u(x,t)\int_0^{+\infty}\frac{1}{\tau}e^{-s\left(\lambda_n+\frac{1}{\tau}+d_{22}\mu_n\right)}ds. \tag{2.5}$$

In the following, we denote the set of positive integers by $\mathbb{N}$ and $\mathbb{N}_0 = \mathbb{N}\cup\{0\}$. Now, the characteristic equation of system (2.2) at $E_*$ is

$$\lambda^2 - \widetilde{T}_n\left(e^{-\lambda\sigma}\right)\lambda + \widetilde{J}_n\left(e^{-\lambda\sigma}\right) - d_{21}v_*\alpha_{12}\mu_n\int_0^{+\infty}\frac{1}{\tau}e^{-s\left(\lambda+\frac{1}{\tau}+d_{22}\mu_n\right)}ds = 0, n \in \mathbb{N}_0, \tag{2.6}$$

where

$$\begin{aligned}\widetilde{T}_n\left(e^{-\lambda\sigma}\right) &= (\alpha_{11}+\alpha_1)-(d_{11}+d_{22})\mu_n+\alpha_2 e^{-\lambda\sigma},\\ \widetilde{J}_n\left(e^{-\lambda\sigma}\right) &= d_{11}d_{22}\mu_n^2-(d_{11}\alpha_1+d_{22}\alpha_{11})\mu_n+\alpha_{11}\alpha_1+e^{-\lambda\sigma}\left(\alpha_2\alpha_{11}-\alpha_{12}\beta_{21}-\alpha_2 d_{11}\mu_n\right).\end{aligned} \tag{2.7}$$

In what follows, we denote $\alpha_{22}=\alpha_1+\alpha_2$ to simplify the equations.

When $d_{11}=d_{22}=d_{21}=\sigma=0$, Eq (2.6) becomes

$$\lambda^2-(\alpha_{11}+\alpha_{22})\lambda+\alpha_{11}\alpha_{22}-\alpha_{12}\beta_{21}=0.$$

When the following condition

$$(H_1)\quad \alpha_{11}+\alpha_{22}<0, \alpha_{11}\alpha_{22}-\alpha_{12}\beta_{21}>0$$

holds, the corresponding ordinary differential equations (ODEs) of system (1.2) at $E_*$ are locally asymptotically stable.

When $d_{11}\neq 0$, $d_{22}\neq 0$, $d_{21}\neq 0$, and $\sigma=0$, Eq (2.6) becomes

$$\lambda^2-T_n\lambda+J_n-d_{21}v_*\alpha_{12}\mu_n\int_0^{+\infty}\frac{1}{\tau}e^{-s\left(\lambda+\frac{1}{\tau}+d_{22}\mu_n\right)}ds=0,$$

where

$$\begin{aligned}T_n &\overset{\Delta}{=} \widetilde{T}_n(1)=\alpha_{11}+\alpha_{22}-(d_{11}+d_{22})\mu_n,\\ J_n &\overset{\Delta}{=} \widetilde{J}_n(1)=d_{11}d_{22}\mu_n^2-(d_{11}\alpha_{22}+d_{22}\alpha_{11})\mu_n+\alpha_{11}\alpha_{22}-\alpha_{12}\beta_{21}.\end{aligned} \tag{2.8}$$

Through calculation, it can be concluded that when

$$(H_2)\quad d_{11}\alpha_{22}+d_{22}\alpha_{11}<2\sqrt{d_{11}d_{22}\left(\alpha_{11}\alpha_{22}-\alpha_{12}\beta_{21}\right)}$$

holds, $J_n>0$ for any $n\in\mathbb{N}_0$. It immediately follows from (2.8) that $T_n<0$ and $J_n>0$ for any $n\in\mathbb{N}_0$ with the conditions $(H_1)$ and $(H_2)$. The condition $(H_2)$ further confirms that the equilibrium $E_*$ without memory-driven diffusion ($d_{21}=0$) is asymptotically stable. That is to say, there is no random-diffusion-driven Turing instability without the gestation delay.

### *2.1. Stability analysis of system (1.2) for $d_{21}\neq 0$, $\sigma=0$ and $\tau=0$*

For $d_{21}\neq 0$, $\sigma=0$, and $\tau=0$, Eq (2.6) becomes

$$\lambda^2-T_n\lambda+J_n-d_{21}v_*\alpha_{12}\mu_n=0,$$

where

$$\lim_{\tau\to 0^+}\int_0^{+\infty}\frac{1}{\tau}e^{-s\left(\lambda_n+\frac{1}{\tau}+d_{22}\mu_n\right)}ds\overset{\varsigma=s/\tau}{=}\lim_{\tau\to 0^+}\int_0^{+\infty}e^{-\tau\varsigma(\lambda_n+d_{22}\mu_n)}e^{-\varsigma}d\varsigma=\int_0^{+\infty}e^{-\varsigma}d\varsigma=1.$$

Thus, there exists

$$d_{21,n}^S=\frac{J_n}{\alpha_{12}v_*\mu_n}<0, n\in\mathbb{N} \tag{2.9}$$

such that $J_n-d_{21}v_*\alpha_{12}\mu_n>0$ for $d_{21}>d_{21,n}^S$ and $J_n-d_{21}v_*\alpha_{12}\mu_n\leq 0$ for $d_{21}\leq d_{21,n}^S$. We therefore present the following theorem.

**Theorem 2.1.** Conditions $(H_1)$ and $(H_2)$ are satisfied, when $\sigma=0$ and $\tau=0$, then the positive equilibrium $E_*$ of system (1.2) is asymptotically stable for $d_{21}>d_{21,n}^S$.

*2.2. Stability analysis of system* (1.2) *for* $d_{21} \neq 0$, $\sigma = 0$ *and* $\tau > 0$

For $d_{21} \neq 0$, $\sigma \geq 0$, and $\tau > 0$, we obtain

$$\int_0^{+\infty} \frac{1}{\tau} e^{-s\left(\lambda_n + \frac{1}{\tau} + d_{22}\mu_n\right)} ds = \begin{cases} \frac{1}{1+\lambda\tau+d_{22}\mu_n\tau}, & Re\lambda + \frac{1}{\tau} + d_{22}\mu_n > 0, \\ +\infty, & Re\lambda + \frac{1}{\tau} + d_{22}\mu_n \leq 0, \end{cases}$$

which means that Eq (2.6) has no roots if $Re\lambda + \frac{1}{\tau} + d_{22}\mu_n \leq 0$. For $Re\lambda + \frac{1}{\tau} + d_{22}\mu_n > 0$, Eq (2.6) is equivalent to the following equation:

$$E_n(\tau, \sigma, \lambda) := \lambda^3 + P_n\left(\tau, e^{-\lambda\sigma}\right)\lambda^2 + Q_n\left(\tau, e^{-\lambda\sigma}\right)\lambda + R_n\left(\tau, e^{-\lambda\sigma}\right) = 0, n \in \mathbb{N}_0, \tag{2.10}$$

where

$$\begin{aligned} P_n\left(\tau, e^{-\lambda\sigma}\right) &= \frac{1}{\tau} + d_{22}\mu_n - \widetilde{T}_n\left(e^{-\lambda\sigma}\right), \\ Q_n\left(\tau, e^{-\lambda\sigma}\right) &= \widetilde{J}_n\left(e^{-\lambda\sigma}\right) - \widetilde{T}_n\left(e^{-\lambda\sigma}\right)\left(\frac{1}{\tau} + d_{22}\mu_n\right), \\ R_n\left(\tau, e^{-\lambda\sigma}\right) &= \widetilde{J}_n\left(e^{-\lambda\sigma}\right)\left(\frac{1}{\tau} + d_{22}\mu_n\right) - \frac{d_{21}v_*\alpha_{12}\mu_n}{\tau}, \end{aligned} \tag{2.11}$$

and $\widetilde{T}_n\left(e^{-\lambda\sigma}\right)$, $\widetilde{J}_n\left(e^{-\lambda\sigma}\right)$ are defined by (2.7).

For $d_{21} \neq 0$, $\sigma = 0$, and $\tau > 0$, Eq (2.10) becomes

$$\lambda^3 + P_n(\tau, 1)\lambda^2 + Q_n(\tau, 1)\lambda + R_n(\tau, 1) = 0, n \in \mathbb{N}, \tag{2.12}$$

where $P_n(\tau, 1) = \frac{1}{\tau} + d_{22}\mu_n - T_n > 0$, $Q_n(\tau, 1) = J_n - T_n\left(\frac{1}{\tau} + d_{22}\mu_n\right) > 0$, and $R_n(\tau, 1) = \frac{J_n - d_{21}v_*\alpha_{12}\mu_n}{\tau} + J_n d_{22}\mu_n$. By the Routh-Hurwitz criterion, we obtain the following lemma.

**Lemma 2.2.** Under conditions $(H_1)$ and $(H_2)$, for fixed $n$,

(I) when $0 < R_n(\tau, 1) < P_n(\tau, 1)Q_n(\tau, 1)$, all roots of Eq (2.12) have negative real part;

(II) when $R_n(\tau, 1) = 0$, Eq (2.12) has a zero root of multiplicity one and two roots with negative real part;

(III) when $R_n(\tau, 1) < 0$, Eq (2.12) has at least one positive real root;

(IV) when $R_n(\tau, 1) = P_n(\tau, 1)Q_n(\tau, 1)$, Eq (2.12) has a pair of purely imaginary $\pm i\sqrt{Q_n(\tau, 1)}$ and a negative real root;

(V) when $R_n(\tau, 1) > P_n(\tau, 1)Q_n(\tau, 1)$, Eq (2.12) has a negative real root and a pair of conjugate complex roots with positive real part.

2.2.1. Stability and Turing bifurcation when $\sigma = 0, \tau > 0$

For any $n \in \mathbb{N}_0$, $\lambda = 0$ is a root of the characteristic equation (2.12) when $R_n(\tau, 1) = 0$, which implies $\tau = \tau_n^S$, where

$$\tau_n^S = \frac{d_{21}v_*\alpha_{12}\mu_n - J_n}{d_{22}\mu_n J_n}, n \in \mathbb{N}, \tag{2.13}$$

provided $d_{21} < d_{21,n}^S$. In this case, Eq (2.12) reduces to $\lambda^3 + P_n(\tau, 1)\lambda^2 + Q_n(\tau, 1)\lambda = 0$ for $n \in \mathbb{N}$. Thus, Eq (2.12) has a zero root of multiplicity one and two roots with negative real part because $P_n(\tau, 1) > 0$ and $Q_n(\tau, 1) > 0$.

The following transversality condition is provided at $\tau = \tau_n^S$.

**Lemma 2.3.** Let $\lambda(\tau)$ be a root of the Eq (2.12) around $\tau = \tau_n^S$ and satisfy $\lambda\left(\tau_n^S\right) = 0$, where $\tau_n^S$ is defined by (2.13). Hence

$$\left.\frac{\mathrm{d}\lambda\left(\tau_n^S\right)}{\mathrm{d}\tau}\right|_{\tau=\tau_n^S} < 0.$$

**Proof.** Taking $\lambda$ as the function of $\tau$ and differentiating of Eq (2.12) with respect to $\tau$, we get

$$\frac{\mathrm{d}\lambda(\tau)}{\mathrm{d}\tau} = -\frac{P_n'(\tau,1)\lambda^2 + Q_n'(\tau,1)\lambda + R_n'(\tau,1)}{3\lambda^2 + 2P_n(\tau,1)\lambda + Q_n(\tau,1)}, \tag{2.14}$$

where $\left.\frac{\mathrm{d}\lambda(\tau)}{\mathrm{d}\tau}\right|_{\tau=\tau_n^S} = -\frac{R_n'\left(\tau_n^S,1\right)}{Q_n\left(\tau_n^S,1\right)} = -\frac{d_{22}\mu_n J_n}{\tau_n^S Q_n\left(\tau_n^S,1\right)} < 0$ because $J_n > 0, \tau_n^S > 0$, and $Q_n\left(\tau_n^S,1\right) > 0$. This compeltes the proof.

Next, we analyze how the root distribution of the characteristic equation (2.12) varies with $d_{21}$.

**Lemma 2.4.** Suppose that conditions $(H_1)$ and $(H_2)$ are satisfied, and $d_{21,n}^S$, $\tau_n^S$ are defined as in (2.9) and (2.13), respectively. Additionally, define

$$d_S^* = \max_{n\in\mathbb{N}}\left\{d_{21,n}^S\right\}, \quad \tau_S = \max_{n\in S_T(d_{21})}\left\{\tau_n^S\right\} \tag{2.15}$$

with

$$S_T(d_{21}) = \left\{n \in \mathbb{N} \mid d_{21,n}^S > d_{21}\right\}, for \text{ fixed } d_{21} < d_S^*. \tag{2.16}$$

Thus, we establish the following results.

(I) When $d_S^* < d_{21} \le 0$, for any $\tau > 0$ and any $n \in \mathbb{N}$, all roots of Eq (2.12) possess negative real parts.

(II) When $d_{21} < d_S^*$, the following subcases hold:

(i) for $\tau > \tau_S$ and any $n \in \mathbb{N}$, all roots of Eq (2.12) possess negative real parts;

(ii) for $0 \le \tau < \tau_S$ and some $n \in S_T(d_{21})$, Eq (2.12) has at least one root with a positive real part;

(iii) $\lambda = 0$ is a root of Eq (2.12) if and only if $\tau = \tau_n^S$ for some $n \in S_T(d_{21})$, and all other roots of Eq (2.12) have negative real parts.

**Proof.** First, we investigate the existence conditions for $d_S^*$ and $\tau_S$. From (2.9), we get

$$d_{21,n}^S = \frac{1}{v_*\alpha_{12}}\left(d_{11}d_{22}\mu_n + \frac{\alpha_{11}\alpha_{22} - \alpha_{12}\beta_{21}}{\mu_n} - (d_{11}\alpha_{22} + d_{22}\alpha_{11})\right),$$

where $\mu_n$ is an increasing function of $n$, and $\lim_{n\to+\infty}\mu_n = +\infty$. Consequently, $d_{21,n}^S$ decreases for $\mu_n > \sqrt{\frac{\alpha_{11}\alpha_{22}-\alpha_{12}\beta_{21}}{d_{11}d_{22}}}$ but increases for $\mu_n < \sqrt{\frac{\alpha_{11}\alpha_{22}-\alpha_{12}\beta_{21}}{d_{11}d_{22}}}$ and $\lim_{n\to+\infty} d_{21,n}^S = -\infty$, which implies that $d_S^* = \max_{n\in\mathbb{N}}\left\{d_{21,n}^S\right\}$ exists. Then, for fixed $d_{21}$, the set $S_T(d_{21})$ defined by (2.16) is finite, which in turn implies the existence of $\tau_S = \max_{n\in S_T(d_{21})}\left\{\tau_n^S\right\}$.

Subsequently, we establish the distribution of the roots of Eq (2.12). For fixed $n$, we have

$$R_n(\tau,1)\begin{cases} < 0, & d_{21} < d_{21,n}^S, 0 \le \tau < \tau_n^S, \\ = 0, & d_{21} < d_{21,n}^S, \tau = \tau_n^S, \\ > 0, & d_{21} > d_{21,n}^S, \forall\tau \ge 0 \text{ or } d_{21} < d_{21,n}^S, \tau > \tau_n^S. \end{cases} \tag{2.17}$$

If $d_{21} \leq 0$ from (2.11), together with $T_n < 0$, $J_n > 0$ and $\alpha_{12} < 0$, we obtain $P_n(\tau,1)Q_n(\tau,1) - R_n(\tau,1) > 0$. Thus, together with (2.17), for fixed $n$, we get

$$\begin{cases} R_n(\tau,1) < 0, & d_{21} < d_{21,n}^S, 0 \leq \tau < \tau_n^S, \\ R_n(\tau,1) = 0, & d_{21} < d_{21,n}^S, \tau = \tau_n^S, \\ 0 < R_n(\tau,1) < P_n(\tau,1)Q_n(\tau,1), & d_{21,n}^S < d_{21} \leq 0, \forall \tau \geq 0 \text{ or } d_{21} < d_{21,n}^S, \tau > \tau_n^S. \end{cases} \tag{2.18}$$

Together with Lemma 2.2, we complete the proof.

**Theorem 2.5.** Given that conditions $(H_1)$ and $(H_2)$ are satisfied, $\tau_n^S$, $d_S^*$, $\tau_S$, and $S_T(d_{21})$ are defined by (2.13), (2.15), and (2.16), respectively. Then, the following statements can be obtained.

(I) If $d_S^* < d_{21} \leq 0$, then the positive equilibrium $E_*$ of system (1.2) is locally asymptotically stable for any $\tau > 0$ and any $n \in \mathbb{N}$;

(II) If $d_{21} < d_S^*$, then the positive equilibrium $E_*$ of system (1.2) is locally asymptotically stable for $\tau > \tau_S$ and unstable for $0 \leq \tau < \tau_S$, and the Turing bifurcations occur at $\tau = \tau_n^S$ for $n \in S_T(d_{21})$.

### 2.2.2. Stability and Hopf bifurcation when $\sigma = 0, \tau > 0$

From Lemma 2.2, it can be seen that when $P_n(\tau,1)Q_n(\tau,1) - R_n(\tau,1) = 0$, the characteristic equation (2.12) has a purely imaginary roots for any $n \in \mathbb{N}_0$. From (2.11), we have

$$\begin{aligned} &P_n(\tau,1)Q_n(\tau,1) - R_n(\tau,1) \\ =&\frac{\left(-T_nJ_n + d_{22}\mu_nT_n^2 - d_{22}^2\mu_n^2T_n\right)\tau^2 + \left(T_n^2 - 2d_{22}\mu_nT_n + d_{21}v_*\alpha_{12}\mu_n\right)\tau - T_n}{\tau^2}. \end{aligned} \tag{2.19}$$

Here, $-T_nJ_n + d_{22}\mu_nT_n^2 - d_{22}^2\mu_n^2T_n > 0$, and $-T_n > 0$.

**Proposition 2.6.** Assume the conditions $(H_1)$ and $(H_2)$ hold, for fixed $n$, $\tau_n^{\pm}$ and $\tau_n$ are defined by (2.21) and (2.24), and $d_{21,n}^H$ is defined by (2.23). Thus, we get

$$\begin{cases} P_n(\tau,1)Q_n(\tau,1) > R_n(\tau,1) > 0, & 0 \leq d_{21} < d_{21,n}^H, \forall \tau \geq 0 \\ & \text{or } d_{21} > d_{21,n}^H, \tau \in [0,\tau_n^+) \cup (\tau_n^-, +\infty) \\ & \text{or } d_{21} = d_{21,n}^H, \tau \in [0,\tau_n) \cup (\tau_n, \infty), \\ P_n(\tau,1)Q_n(\tau,1) = R_n(\tau,1), & d_{21} = d_{21,n}^H, \tau = \tau_n \text{ or } d_{21} > d_{21,n}^H, \tau = \tau_n^{\pm}, \\ P_n(\tau,1)Q_n(\tau,1) < R_n(\tau,1), & d_{21} > d_{21,n}^H, \tau \in (\tau_n^+, \tau_n^-). \end{cases}$$

**Proof.** From Eq (2.19), if $T_n^2 - 2d_{22}\mu_nT_n + d_{21}v_*\alpha_{12}\mu_n = 0$, then we have

$$\tilde{d}_{21} = \frac{-T_n^2 + 2d_{22}\mu_nT_n}{v_*\alpha_{12}\mu_n} > 0. \tag{2.20}$$

(I) If $d_{21} \leq \widetilde{d}_{21}$, we obtain $T_n^2 - 2d_{22}\mu_nT_n + d_{21}v_*\alpha_{12}\mu_n > 0$ for any $\tau \geq 0$, thus $P_n(\tau,1)Q_n(\tau,1) - R_n(\tau,1) > 0$.

(II) If $d_{21} > \widetilde{d}_{21}$, then $T_n^2 - 2d_{22}\mu_nT_n + d_{21}v_*\alpha_{12}\mu_n < 0$. Thus, we can get

$$P_n(\tau,1)Q_n(\tau,1) - R_n(\tau,1) > 0 \Longleftrightarrow \Delta_n > 0, \tau \in [0,\tau_n^+) \cup (\tau_n^-, +\infty) \text{ or } \Delta_n < 0, \tau \geq 0,$$

where

$$\tau_n^{\pm} = \frac{T_n^2 - 2d_{22}\mu_nT_n + d_{21}v_*\alpha_{12}\mu_n \pm \sqrt{\Delta_n}}{2T_nJ_n - 2d_{22}\mu_nT_n^2 + 2d_{22}^2\mu_n^2T_n}, 0 < \tau_n^+ < \tau_n^-, \tag{2.21}$$

with

$$\Delta_n = \left(T_n^2 - 2d_{22}\mu_n T_n + d_{21}v_*\alpha_{12}\mu_n\right)^2 - 4T_n^2\left(J_n - d_{22}\mu_n T_n + d_{22}^2\mu_n^2\right).$$

(i) When $\Delta_n < 0$ is equivalent to $\hat{d}_{21} < d_{21} < d_{21,n}^H$,

$$\hat{d}_{21} = \frac{-T_n^2 + 2d_{22}\mu_n T_n - 2T_n\sqrt{J_n - d_{22}\mu_n T_n + d_{22}^2\mu_n^2}}{v_*\alpha_{12}\mu_n}, \tag{2.22}$$

and

$$d_{21,n}^H = \frac{-T_n^2 + 2d_{22}\mu_n T_n + 2T_n\sqrt{J_n - d_{22}\mu_n T_n + d_{22}^2\mu_n^2}}{v_*\alpha_{12}\mu_n} > 0. \tag{2.23}$$

It follows from (2.20), (2.22), and (2.23) that $\hat{d}_{21} < \widetilde{d}_{21} < d_{21,n}^H$ because $T_n < 0$, $\alpha_{12} < 0$. Thus, when $\widetilde{d}_{21} < d_{21} < d_{21,n}^H$, $P_n(\tau,1)Q_n(\tau,1) - R_n(\tau,1) > 0$ for any $\tau \geq 0$.

Combining the results of (I) and case (i) in (II), we deduce when $d_{21} < d_{21,n}^H$, $P_n(\tau,1)Q_n(\tau,1) - R_n(\tau,1) > 0$ for any $\tau \geq 0$.

(ii) When $\Delta_n > 0$ is equivalent to $d_{21} > d_{21,n}^H$, then $P_n(\tau,1)Q_n(\tau,1) - R_n(\tau,1) = 0$ if $\tau = \tau_n^{\pm}$, and $P_n(\tau,1)Q_n(\tau,1) - R_n(\tau,1) < 0$ if $\tau \in (\tau_n^+, \tau_n^-)$, and $P_n(\tau,1)Q_n(\tau,1) - R_n(\tau,1) > 0$ if $\tau \in [0,\tau_n^+) \cup (\tau_n^-, +\infty)$.

(iii) When $\Delta_n = 0$, then $d_{21} = d_{21,n}^H$, denote

$$\tau_n = \frac{T_n^2 - 2d_{22}\mu_n T_n + d_{21}v_*\alpha_{12}\mu_n}{2T_n J_n - 2d_{22}\mu_n T_n^2 + 2d_{22}^2\mu_n^2 T_n}. \tag{2.24}$$

Thus, we get $P_n(\tau,1)Q_n(\tau,1) - R_n(\tau,1) = 0$ if $\tau = \tau_n$, and $P_n(\tau,1)Q_n(\tau,1) - R_n(\tau,1) > 0$ if $\tau \neq \tau_n$.

If $d_{21} \geq 0$, together with $J_n > 0$ and $\alpha_{12} < 0$, then $R_n(\tau,1) = \frac{J_n - d_{21}v_*\alpha_{12}\mu_n}{\tau} + J_n d_{22}\mu_n > 0$. Further, we obtain

$$\begin{cases} P_n(\tau,1)Q_n(\tau,1) > R_n(\tau,1) > 0, & 0 \leq d_{21} < d_{21,n}^H, \forall \tau \geq 0 \\ & \text{or } d_{21} > d_{21,n}^H, \tau \in [0,\tau_n^+) \cup (\tau_n^-, +\infty) \\ & \text{or } d_{21} = d_{21,n}^H, \tau \in [0,\tau_n) \cup (\tau_n, \infty), \\ P_n(\tau,1)Q_n(\tau,1) = R_n(\tau,1), & d_{21} = d_{21,n}^H, \tau = \tau_n \text{ or } d_{21} > d_{21,n}^H, \tau = \tau_n^{\pm}, \\ P_n(\tau,1)Q_n(\tau,1) < R_n(\tau,1), & d_{21} > d_{21,n}^H, \tau \in (\tau_n^+, \tau_n^-). \end{cases}$$

We have completed the proof.

Next, together with Lemma 2.2, we get the distribution of the roots of Eq (2.12) for $d_{21} \geq 0$.

**Lemma 2.7.** Suppose that conditions $(H_1)$ and $(H_2)$ are satisfied. $\tau_n^{\pm}$, $d_{21,n}^H$, and $\tau_n$ are defined according to (2.21), (2.23), and (2.24), respectively. For a given fixed $n$, we get the results as follows.

(I) When $0 \leq d_{21} < d_{21,n}^H$, all roots of Eq (2.12) have negative real parts for any $\tau > 0$.

(II) When $d_{21} = d_{21,n}^H$, all roots of Eq (2.12) have negative real parts for $\tau \neq \tau_n$, and Eq (2.12) has one negative root and a pair of purely imaginary roots $\pm i\omega_n$ at $\tau = \tau_n$, where

$$\omega_n = \sqrt{Q_n(\tau_n,1)} = \sqrt{J_n - T_n\left(\frac{1}{\tau_n} + d_{22}\mu_n\right)}. \tag{2.25}$$

(III) When $d_{21} > d_{21,n}^H$, all roots of Eq (2.12) have negative real parts for $\tau \in [0, \tau_n^+) \cup (\tau_n^-, +\infty)$; at least one root of all roots of Eq (2.12) has positive real part for $\tau \in (\tau_n^+, \tau_n^-)$; Eq (2.12) has one negative root and a pair of purely imaginary roots $\pm i\omega_n^+$ $(\pm i\omega_n^-)$ at $\tau = \tau_n^+$ $(\tau = \tau_n^-)$, where

$$\omega_n^{\pm} = \sqrt{Q_n(\tau_n^{\pm}, 1)} = \sqrt{J_n - T_n\left(\frac{1}{\tau_n^{\pm}} + d_{22}\mu_n\right)}. \tag{2.26}$$

The following transversality conditions are provided for the purely imaginary roots of Eq (2.12) at $\tau = \tau_n, \tau_n^{\pm}$.

**Lemma 2.8.** Suppose $\lambda(\tau) = \alpha(\tau) \pm i\beta(\tau)$ are a pair of conjugate complex roots of Eq (2.12) around $\tau = \tau_n, \tau_n^{\pm}$ which satisfy $\alpha(\tau_n, \tau_n^{\pm}) = 0, \beta(\tau_n) = \omega_n$, and $\beta(\tau_n^{\pm}) = \omega_n^{\pm}$, where $\tau_n^{\pm}, \tau_n$ and $\omega_n, \omega_n^{\pm}$ are defined by (2.21), (2.24), (2.25), and (2.26), respectively. Then we have

$$\left.\frac{\mathrm{d}\,\mathrm{Re}(\lambda(\tau))}{\mathrm{d}\tau}\right|_{\tau=\tau_n} = 0, \quad \left.\frac{\mathrm{d}\,\mathrm{Re}(\lambda(\tau))}{\mathrm{d}\tau}\right|_{\tau=\tau_n^+} > 0, \quad \left.\frac{\mathrm{d}\,\mathrm{Re}(\lambda(\tau))}{\mathrm{d}\tau}\right|_{\tau=\tau_n^-} < 0.$$

**Proof.** From (2.14), we get that

$$\frac{\mathrm{d}\lambda}{\mathrm{d}\tau} = \frac{\frac{1}{\tau^2}(\lambda^2 - T_n\lambda + J_n - d_{21}v_*\alpha_{12}\mu_n)}{3\lambda^2 + 2\left(\frac{1}{\tau} + d_{22}\mu_n - T_n\right)\lambda + J_n - T_n\left(\frac{1}{\tau} + d_{22}\mu_n\right)}.$$

From (2.11), we have

$$\tau_n = \frac{1}{\sqrt{J_n - d_{22}\mu_n T_n + d_{22}^2\mu_n^2}}, \tau_n^+ < \frac{1}{\sqrt{J_n - d_{22}\mu_n T_n + d_{22}^2\mu_n^2}}, \tau_n^- > \frac{1}{\sqrt{J_n - d_{22}\mu_n T_n + d_{22}^2\mu_n^2}}$$

by the Vieta's formulas. Therefore,

$$\left(\mathrm{Re}\left(\frac{\mathrm{d}\lambda}{\mathrm{d}\tau}\right)\right)\Big|_{\tau=\tau_n,\tau_n^{\pm}} = \frac{T_n\left(\tau^2\left(J_n - d_{22}\mu_n T_n + d_{22}^2\mu_n^2\right) - 1\right)}{2\tau^3\left(\omega^2 + \left(\frac{1}{\tau} - T_n\right)^2\right)} \begin{cases} = 0, & \tau = \tau_n, \omega = \omega_n, \\ > 0, & \tau = \tau_n^+, \omega = \omega_n^+, \\ < 0, & \tau = \tau_n^-, \omega = \omega_n^-. \end{cases}$$

By combining with the fact

$$\frac{\mathrm{d}\,\mathrm{Re}(\lambda(\tau))}{\mathrm{d}\tau} = \mathrm{Re}\left(\frac{\mathrm{d}\lambda(\tau)}{\mathrm{d}\tau}\right),$$

we have completed the proof.

Now, we will study the monotonicity of the function $d_{21,n}^H$ in the following two steps.

**Step 1.** From (2.20) and (2.23), we rewrite $d_{21,n}^H$ as $d_{21,n}^H = \widetilde{d}_{21} + H(\mu_n)$, where

$$H(\mu_n) = \frac{2T_n\sqrt{J_n - d_{22}\mu_n T_n + d_{22}^2\mu_n^2}}{v_*\alpha_{12}\mu_n}. \tag{2.27}$$

Then, we rewrite $\widetilde{d}_{21}$ as $\widetilde{d}_{21} = \widetilde{d}_{21}^{(1)} + \widetilde{d}_{21}^{(2)}$, where $\widetilde{d}_{21}^{(1)} = \frac{-T_n^2}{v_*\alpha_{12}\mu_n}$ and $\widetilde{d}_{21}^{(2)} = \frac{2d_{22}T_n}{v_*\alpha_{12}}$. Clearly, the function

$$\widetilde{d}_{21}^{(1)} = -\frac{1}{v_*\alpha_{12}}\left(\frac{(\alpha_{11} + \alpha_{22})^2}{\mu_n} + (d_{11} + d_{22})^2\mu_n - 2(d_{11} + d_{22})(\alpha_{11} + \alpha_{22})\right)$$

is decreasing when $\mu_n < -\frac{\alpha_{11}+\alpha_{22}}{d_{11}+d_{22}}$ and increasing when $\mu_n > -\frac{\alpha_{11}+\alpha_{22}}{d_{11}+d_{22}}$. Meanwhile, the function $\widetilde{d}_{21}^{(2)} = \frac{2d_{22}T_n}{v_*\alpha_{12}}$ increases for any $\mu_n \geq 0$, which implies that

$$\frac{\mathrm{d}\widetilde{d}_{21}}{\mathrm{d}\mu_n} > 0, for \quad \mu_n > -\frac{\alpha_{11}+\alpha_{22}}{d_{11}+d_{22}}. \tag{2.28}$$

**Step 2.** Next, we have the following result, which is similar to Proposition 2.6 in [25]. Assume that the conditions $(H_1)$ and $(H_2)$ are satisfied, there exists a number $\mu_* > 0$ such that $\frac{\mathrm{d}H(\mu)}{\mathrm{d}\mu_n} > 0$, for $\mu_n > \mu_*$, where $\mu_*$ is the maximum positive real root of $h(\mu_n)$, and

$$h(\mu_n) = a_h\mu_n^3 + b_h\mu_n^2 + c_h\mu_n + d_h, \tag{2.29}$$

with

$$\begin{aligned} &a_h = 4d_{22}(d_{11}+d_{22})^2 > 0, b_h = -(d_{11}+d_{22})(d_{11}\alpha_{22}+d_{22}\alpha_{11}+d_{22}(\alpha_{11}+\alpha_{22})),\\ &c_h = -(\alpha_{11}+\alpha_{22})(d_{11}\alpha_{22}+d_{22}\alpha_{11}+d_{22}(\alpha_{11}+\alpha_{22})), d_h = 2(\alpha_{11}+\alpha_{22})(\alpha_{11}\alpha_{22}-\alpha_{12}\beta_{21}) < 0. \end{aligned}$$

Then, we obtain that $d_{21,n}^H$ is monotonically increasing with respect to $\mu_n$ when $\mu_n > \max\left\{-\frac{\alpha_{11}+\alpha_{22}}{d_{11}+d_{22}}, \mu_*\right\}$. Therefore, we denote

$$\hat{n} = \min\left\{n \in \mathbb{N} \,\middle|\, \mu_n > \max\left\{-\frac{\alpha_{11}+\alpha_{22}}{d_{11}+d_{22}}, \mu_*\right\}\right\}, \tag{2.30}$$

and

$$d_H^* = \min_{n\in\mathbb{N}}\left\{d_{21,n}^H\right\} = \min_{1\leq n\leq\hat{n}}\left\{d_{21,n}^H\right\}. \tag{2.31}$$

For fixed $d_{21} > d_H^*$, let

$$S_H(d_{21}) = \left\{n \in \mathbb{N} \mid d_{21,n}^H < d_{21}\right\}, \tag{2.32}$$

which is a finite set in terms of the property of $d_{21,n}^H$ and also

$$\tau_* = \min_{n\in S_H(d_{21})}\tau_n^+, \quad \tau^* = \max_{n\in S_H(d_{21})}\tau_n^-. \tag{2.33}$$

**Theorem 2.9.** Suppose that conditions $(H_1)$ and $(H_2)$ are satisfied. $d_H^*$, $S_H(d_{21})$, $\tau_*$, and $\tau^*$ are defined by (2.31), (2.32), and (2.33), respectively. Then, we can derive the following results.

(I) When $0 \leq d_{21} < d_H^*$, for $\forall\tau > 0$ and any $n \in \mathbb{N}$, all roots of Eq (2.12) have negative real parts, then the positive equilibrium $E_*$ of system (1.2) is locally asymptotically stable;

(II) When $d_{21} > d_H^*$, the following subcases hold:

(i) for $\tau \in [0, \tau_*) \cup (\tau^*, +\infty)$ and any $n \in \mathbb{N}$, all roots of Eq (2.12) have negative real parts. Thus, the positive equilibrium $E_*$ of system (1.2) is locally asymptotically stable;

(ii) for $\tau_* < \tau < \tau^*$ and some $n \in S_H(d_{21})$, at least one root of Eq (2.12) has positive real part. Then the positive equilibrium $E_*$ of system (1.2) is unstable;

(iii) for $\tau = \tau_n^{\pm}$ and some $n \in S_H(d_{21})$, Eq (2.12) has a pair of purely imaginary roots, and all other roots of Eq (2.12) have negative real parts. Thus, system (1.2) undergoes Hopf bifurcation at $E_*$.

*2.3. Stability and bifurcation analysis when $d_{21} \neq 0$, $\tau \geq 0$, and $\sigma \geq 0$*

By Eq (2.10), it can be seen that regardless of whether $\sigma = 0$ or $\sigma > 0$, if $\lambda = 0$ is the root of Eq (2.10), then $R(\tau, 1) = 0$. That is to say, the gestation delay $\sigma$ does not influence the presence of the zero root in the characteristic equation (2.10). Therefore, in this subsection, we concentrate our efforts on exploring whether there exist purely imaginary roots for Eq (2.10) when $\sigma > 0$. First, we have the following lemma.

**Lemma 2.10.** Fix $d_{21} < d_S^*$, the positive equilibrium $E_*$ of system (1.2) is unstable for all $0 \leq \tau < \tau_S$ and $\sigma \geq 0$. When $d_{21} > d_S^*$ , Eq (2.10) has no zero roots for all $\tau \geq 0$ and $\sigma \geq 0$.

**Proof.** For fixed $n \in \mathbb{N}$, define $\mathcal{F} : \mathbb{R} \to \mathbb{R}$ as the function of $\lambda_n$:

$$\mathcal{F}(\lambda_n) = \lambda_n^3 + P_n\left(\tau, e^{-\lambda_n\sigma}\right)\lambda_n^2 + Q_n\left(\tau, e^{-\lambda_n\sigma}\right)\lambda_n + R_n\left(\tau, e^{-\lambda_n\sigma}\right), \lambda_n \in \mathbb{R}.$$

Eq (2.10) is equivalent to $\mathcal{F}(\lambda_n) = 0$.

(i) From (2.17), if $0 \leq \tau < \tau_n^S$ and $d_{21} < d_{21,n}^S$, then $\mathcal{F}(0) = R_n(\tau, 1) < 0$ and $\lim_{\lambda_n \to +\infty} \mathcal{F}(\lambda_n) = +\infty$, and Eq (2.10) has at least one positive real root. Therefore, for fixed $d_{21} < d_S^*$, in terms of $\tau_S = \max_{n \in S_T(d_{21})}\left\{\tau_n^S\right\}$, where $S_T(d_{21}) = \left\{n \in \mathbb{N} \mid d_{21,n}^S > d_{21}\right\}$, Eq (2.10) has infinitely many positive real roots for $d_{21} < d_S^*$, $0 \leq \tau < \tau_S$, and $\sigma \geq 0$.

(ii) From (2.17), $R_n(\tau, 1) = 0$ if and only if $\tau = \tau_n^S$ $(d_{21} < d_{21,n}^S)$. Thus, if $\lambda_n = 0$ is a root of $\mathcal{F}(\lambda_n) = 0$, then $\mathcal{F}(0) = R_n(\tau, 1) = 0$ if and only if $\tau = \tau_n^S$ ( $d_{21} < d_{21,n}^S$). This implies that Eq (2.10) has no zero roots for all $d_{21} > d_S^*$ and $\tau \geq 0, \sigma \geq 0$. This completes the proof.

Now, we investigate the existence of purely imaginary roots of Eq (2.10) by considering the following two cases:

$$\tau > \tau_S, \sigma > 0 (d_{21} < d_S^*)$$

and

$$\tau > 0, \sigma > 0 (d_{21} > d_S^*),$$

which correspond to the occurrence of Hopf bifurcation in system (1.2).

For convenience, denote

$$P_n\left(\tau, e^{-\lambda\sigma}\right) = p_n - \alpha_2 e^{-\lambda\sigma}, Q_n\left(\tau, e^{-\lambda\sigma}\right) = q_n + g_n e^{-\lambda\sigma}, R_n\left(\tau, e^{-\lambda\sigma}\right) = r_n + b_n e^{-\lambda\sigma}, \tag{2.34}$$

where

$$\begin{aligned}
p_n &= (d_{11} + 2d_{22})\mu_n + \frac{1}{\tau} - (\alpha_1 + \alpha_{11}), g_n = \alpha_2\left(\alpha_{11} - d_{11}\mu_n - d_{22}\mu_n - \frac{1}{\tau}\right) - \alpha_{12}\beta_{21},\\
q_n &= \left(2d_{11}d_{22} + d_{22}^2\right)\mu_n^2 - \left(d_{11}\alpha_1 + d_{22}(2\alpha_{11} + \alpha_1) - \frac{d_{11} + d_{22}}{\tau}\right)\mu_n + \alpha_{11}\alpha_1 - \frac{\alpha_{11} + \alpha_1}{\tau},\\
r_n &= d_{11}d_{22}^2\mu_n^3 - d_{22}\left(d_{22}\alpha_{11} + d_{11}\alpha_1 - \frac{d_{11}}{\tau}\right)\mu_n^2 + \left(d_{22}\alpha_{11}\alpha_1 - \frac{d_{22}\alpha_{11} + d_{11}\alpha_1 + d_{21}v_*\alpha_{12}}{\tau}\right)\mu_n + \frac{\alpha_{11}\alpha_1}{\tau},\\
b_n &= (\alpha_{11}\alpha_2 - \alpha_{12}\beta_{21} - \alpha_2 d_{11}\mu_n)\left(\frac{1}{\tau} + d_{22}\mu_n\right).
\end{aligned} \tag{2.35}$$

Let $\pm iv (v > 0)$ be a pair of roots of Eq (2.10). Separating real and imaginary parts, we obtain

$$\begin{aligned}
g_n v\sin(v\sigma) + \left(\alpha_2 v^2 + b_n\right)\cos(v\sigma) &= p_n v^2 - r_n,\\
g_n v\cos(v\sigma) - \left(\alpha_2 v^2 + b_n\right)\sin(v\sigma) &= v^3 - q_n v.
\end{aligned} \tag{2.36}$$

By the Cramer's rule,

$$\begin{cases} \cos(v\sigma) = \frac{(p_n v^2 - r_n)(\alpha_2 v^2 + b_n) + g_n v(v^3 - q_n v)}{(\alpha_2 v^2 + b_n)^2 + (g_n v)^2}, \\ \sin(v\sigma) = \frac{-(v^3 - q_n v)(\alpha_2 v^2 + b_n) + g_n v(p_n v^2 - r_n)}{(\alpha_2 v^2 + b_n)^2 + (g_n v)^2}. \end{cases} \tag{2.37}$$

Square both sides of (2.36) and add them together, and we obtain the following sixth-degree equation in terms of $v$:

$$v^6 + s_{n,1} v^4 + s_{n,2} v^2 + s_{n,3} = 0, \tag{2.38}$$

where

$$s_{n,1} = p_n^2 - 2q_n - \alpha_2^2, s_{n,2} = q_n^2 - g_n^2 - 2\alpha_2 b_n - 2p_n r_n, s_{n,3} = r_n^2 - b_n^2. \tag{2.39}$$

Let $v^2 = z$, which yields

$$z^3 + s_{n,1} z^2 + s_{n,2} z + s_{n,3} = 0. \tag{2.40}$$

Thus, $\pm iv (v > 0)$ are a pair of purely imaginary roots of Eq (2.10) if and only if $v^2$ is a positive root of Eq (2.40). We analyze when the cubic polynomial (2.40) has positive real roots using the method in [28]. Define:

$$L(z) = z^3 + s_{n,1} z^2 + s_{n,2} z + s_{n,3},$$

and

$$L'(z) = 3z^2 + 2s_{n,1} z + s_{n,2}. \tag{2.41}$$

For fixed $n$, define:

$$z_n^* = \frac{-s_{n,1} + \sqrt{s_{n,1}^2 - 3s_{n,2}}}{3}, \text{if} \quad s_{n,1}^2 - 3s_{n,2} > 0. \tag{2.42}$$

In what follows, we have the distribution of the positive roots of Eq (2.40).

**Lemma 2.11.** Consider Eq (2.40), where $s_{n,k} (k = 1, 2, 3)$ and $z_n^*$ are defined as in (2.39) and (2.42). Thus, for fixed $n$, if $(R_1)\, s_{n,3} \geq 0, s_{n,1}^2 - 3s_{n,2} \leq 0$ holds, then Eq (2.40) has no positive roots; if $(R_2)\, s_{n,3} < 0$ or $(R_3)\, s_{n,3} \geq 0, s_{n,1}^2 - 3s_{n,2} > 0$ and $z_n^* > 0, L(z_n^*) \leq 0$ holds, then Eq (2.40) has at least one positive root.

**Lemma 2.12.** For fixed $\tau$, there exists $N_* \geq 0$ such that Eq (2.40) has no positive roots for $n > N_*$.

**Proof.** From (2.35) and (2.39), $\lim_{n\to+\infty} \mu_n = +\infty$, and treating $\mu_n$ as a continuous variable,

$$\lim_{n\to+\infty} s_{n,1} = \lim_{n\to+\infty} \left(d_{11}^2 + 2d_{22}^2\right)\mu_n^2 = +\infty, \lim_{n\to+\infty} s_{n,3} = \lim_{n\to+\infty} d_{11}^2 d_{22}^4 \mu_n^6 = +\infty,$$
$$\lim_{n\to+\infty} (s_{n,1}s_{n,2} - s_{n,3}) = \lim_{n\to+\infty} \left(\left(d_{11}^2 + 2d_{22}^2\right)\left(2d_{11}^2 d_{22}^2 + d_{22}^4\right) - d_{11}^2 d_{22}^4\right)\mu_n^6 = +\infty.$$

By the Routh-Hurwitz stability criterion, Eq (2.40) has no positive roots for $n > N_*$. This completes the proof.

For fixed $n \in [0, N_*]$, assume that Eq (2.40) has three positive roots $z_{n,1}, z_{n,2}$, and $z_{n,3}$. Then, for the same $n$, Eq (2.38) has three positive roots $v_{n,1} = \sqrt{z_{n,1}}, v_{n,2} = \sqrt{z_{n,2}}$, and $v_{n,3} = \sqrt{z_{n,3}}$. By (2.37), for $k = 1, 2, 3, n \in [0, N_*]$, we denote

$$C_{n,k} := -\left(v_{n,k}^3 - q_n v_{n,k}\right)\left(\alpha_2 v_{n,k}^2 + b_n\right) + g_n v_{n,k}\left(p_n v_{n,k}^2 - r_n\right), \tag{2.43}$$

and its sign is the same as $\sin\left(v_{n,k}\sigma_{n,k}^{(j)}\right)$ $(n \in [0, N_*], j \in \mathbb{N}_0, k = 1, 2, 3)$. Here, $\sigma_{n,k}^{(j)}$ is defined as

$$\sigma_{n,k}^{(j)} = \begin{cases} \frac{1}{v_{n,k}}\left\{\arccos\left(D_{n,k}\right) + 2j\pi\right\}, \text{ if } C_{n,k} \geq 0, \\ \frac{1}{v_{n,k}}\left\{-\arccos\left(D_{n,k}\right) + (2j+1)\pi\right\}, \text{ if } C_{n,k} < 0, \end{cases} \tag{2.44}$$

where

$$D_{n,k} := \frac{\left(p_n v_{n,k}^2 - r_n\right)\left(\alpha_2 v_{n,k}^2 + b_n\right) + g_n v_{n,k}\left(v_{n,k}^3 - q_n v_{n,k}\right)}{\left(\alpha_2 v_{n,k}^2 + b_n\right)^2 + g_n^2 v_{n,k}^2}. \tag{2.45}$$

**Proposition 2.13.** When the positive roots $v_{n,k}$ $(n \in [0, N_*], k = 1, 2, 3)$ of Eq (2.40) exist, then Eq (2.10) has a pair of purely imaginary roots $\pm i v_{n,k}$ at $\sigma = \sigma_{n,k}^{(j)}$, where $\sigma_{n,k}^{(j)}$ is defined as in (2.44).

Because

$$\lim_{j \to +\infty} \sigma_{n,k}^{(j)} = +\infty, k = 1, 2, 3, n \in [0, N_*],$$

for fixed $\tau$, we define

$$\sigma_* = \sigma_{n_*,k_*}^{(0)} = \min_{0 \leq n \leq N_*, k \in \{1,2,3\}, j \in \mathbb{N}_0} \sigma_{n,k}^{(j)}, \quad v_* = v_{n_*,k_*}. \tag{2.46}$$

If Eq (2.40) has a positive root $v^2 (v > 0)$, then when $\sigma = \sigma_{n,k}^{(j)}$, $(n \in [0, N_*], j \in \mathbb{N}_0, k = 1, 2, 3)$, Eq (2.10) has a pair of purely imaginary roots $\pm iv$. Next, we calculate the transversality condition for the occurrence of Hopf bifurcation in system (1.2).

**Lemma 2.14.** Suppose $z_{n,k} = v_{n,k}^2$ and $L'\left(z_{n,k}\right) \neq 0$, where $L'(z)$ is defined by (2.41). Then $iv_{n,k}$ is a simple root of Eq (2.10) for $\sigma = \sigma_{n,k}^{(j)}$, and there exists the unique root $\lambda(\sigma) = \rho(\sigma) + iv(\sigma)$ of Eq (2.10) for $\sigma \in \left(\sigma_{n,k}^{(j)} - \epsilon, \sigma_{n,k}^{(j)} + \epsilon\right)$ and some small enough $\epsilon > 0$ such that $\rho\left(\sigma_{n,k}^{(j)}\right) = 0$ and $v\left(\sigma_{n,k}^{(j)}\right) = v_{n,k}$. Moreover, $\operatorname{sign}\left(\frac{\mathrm{d}\,\mathrm{Re}(\lambda(\sigma))}{\mathrm{d}\sigma}\Big|_{\sigma=\sigma_{n,k}^{(j)}}\right) = \operatorname{sign}\left(L'\left(z_{n,k}\right)\right) \neq 0$.

**Proof.** From (2.34), we rewrite Eq (2.10) as

$$M(\lambda, \sigma) := X(\lambda) + Y(\lambda)e^{-\lambda\sigma} = 0, \tag{2.47}$$

where

$$X(\lambda) = \lambda^3 + p_n\lambda^2 + q_n\lambda + r_n, \quad Y(\lambda) = -\alpha_2\lambda^2 + g_n\lambda + b_n,$$

and $p_n, q_n, g_n, r_n, b_n$ are defined as in (2.35). Then, we obtain

$$\frac{\partial M}{\partial \lambda}(\lambda, \sigma) = e^{-\lambda\sigma}T(\lambda, \sigma) \text{ and } \frac{\partial M}{\partial \sigma}(\lambda, \sigma) = -\lambda e^{-\lambda\sigma}Y(\lambda),$$

where

$$T(\lambda, \sigma) = \left(3\lambda^2 + 2p_n\lambda + q_n\right)e^{\lambda\sigma} - 2\alpha_2\lambda + g_n + \sigma\left(\alpha_2\lambda^2 - g_n\lambda - b_n\right). \tag{2.48}$$

Substituting $\lambda = iv_{n,k}, \sigma = \sigma_{n,k}^{(j)}$ into $T(\lambda, \sigma)$, $Y(\lambda)$, and using (2.36) and (2.39), we get that

$$\begin{aligned}
&\operatorname{Im}\left\{T\left(iv_{n,k}, \sigma_{n,k}^{(j)}\right)\overline{Y\left(iv_{n,k}\right)}\right\} \\
=&g_n v_{n,k}\left\{-(-3v_{n,k}^2 + q_n)\cos(v_{n,k}\sigma_{n,k}^{(j)}) + 2p_n v_{n,k}\sin(v_{n,k}\sigma_{n,k}^{(j)})\right\} - g_n^2 v_{n,k} + \sigma_{n,k}^{(j)}\alpha_2 g_n v_{n,k}^3 - 2\alpha_2 v_{n,k}(\alpha_2 v_{n,k}^2 + b_n) \\
&+ (\alpha_2 v_{n,k}^2 + b_n)\left\{(-3v_{n,k}^2 + q_n)\sin(v_{n,k}\sigma_{n,k}^{(j)}) + 2p_n v_{n,k}\cos(v_{n,k}\sigma_{n,k}^{(j)})\right\} - \sigma_{n,k}^{(j)} g_n v_{n,k}(\alpha_2 v_{n,k}^2 + b_n) + \sigma_{n,k}^{(j)} b_n g_n v_{n,k} \\
=&v_{n,k}\left\{3v_{n,k}^4 + \left(2p_n^2 - 4q_n - 2\alpha_2^2\right)v_{n,k}^2 + \left(q_n^2 - g_n^2 - 2\alpha_2 b_n - 2p_n r_n\right)\right\} \\
=&v_{n,k}\left\{3z_{n,k}^2 + 2s_{n,1}z_{n,k} + s_{n,2}\right\} = v_{n,k}L'\left(z_{n,k}\right).
\end{aligned} \tag{2.49}$$

Then, differentiating Eq (2.47) with respect to $\sigma$, we obtain

$$T(\lambda,\sigma)\frac{\mathrm{d}\lambda(\sigma)}{\mathrm{d}\sigma} = \lambda Y(\lambda).$$

Thus,

$$\frac{\mathrm{d}\lambda(\sigma)}{\mathrm{d}\sigma} = \frac{\lambda Y(\lambda)}{T(\lambda,\sigma)}.$$

It is easy to verify that

$$\begin{aligned}&\operatorname{sign}\left(\frac{\mathrm{d}\operatorname{Re}(\lambda(\sigma))}{\mathrm{d}\sigma}\Big|_{\sigma=\sigma_{n,k}^{(j)}}\right) = \operatorname{sign}\left(\operatorname{Re}\left(\frac{\mathrm{d}(\lambda(\sigma))}{\mathrm{d}\sigma}\right)\Big|_{\sigma=\sigma_{n,k}^{(j)}}\right)\\ &= \operatorname{sign}\left(\operatorname{Im}\left\{T\left(iv_{n,k},\sigma_{n,k}^{(j)}\right)\overline{Y\left(iv_{n,k}\right)}\right\}\right) = \operatorname{sign}\left(L'\left(z_{n,k}\right)\right).\end{aligned}$$

Therefore, $\operatorname{sign}\left(\frac{\mathrm{d}\operatorname{Re}(\lambda(\sigma))}{\mathrm{d}\sigma}\Big|_{\sigma=\sigma_{n,k}^{(j)}}\right) \neq 0$ when $L'(z_{n,k}) \neq 0$. This completes the proof.

When $\sigma = 0$, we see that Eq (2.10) becomes Eq (2.12). From Theorem 2.5 and Theorem 2.9, we conclude that all roots of Eq (2.12) have negative real parts if and only if

$$(d_{21},\tau) \in E_s \cup E_c \cup E_h,$$

where

$$\begin{aligned}E_s &= \left\{(d_{21},\tau) \mid d_{21} < d_S^*, \tau > \tau_S\right\},\\ E_c &= \left\{(d_{21},\tau) \mid d_S^* < d_{21} < d_H^*, \tau \geq 0\right\},\\ E_h &= \left\{(d_{21},\tau) \mid d_{21} > d_H^*, 0 \leq \tau < \tau_*, \tau > \tau^*\right\}.\end{aligned} \tag{2.50}$$

By employing the result derived from Lemmas 2.10–2.12, 2.14 and Proposition 2.13, we obtain the following findings regarding the root distribution of the equation (2.10).

**Theorem 2.15.** Let conditions $(H_1)$ and $(H_2)$ hold, and conditions $(R_1)$, $(R_2)$ and $(R_3)$ are defined as in Lemma 2.11. $d_S^*$, $\tau_S$, and $L'(z)$; $\sigma_{n,k}^{(j)}\,(n \in [0, N_*]\,, j \in \mathbb{N}_0, k = 1, 2, 3)$; $\sigma_*$, and $E_s, E_c, E_h$ are defined by (2.15), (2.41), (2.44), (2.46), and (2.50), respectively. Define

$$E_s^+ = \left\{(d_{21},\tau) \mid d_{21} < d_S^*, 0 \leq \tau < \tau_S\right\}. \tag{2.51}$$

Then, we have following results.

(I) When $(d_{21},\tau) \in E_s \cup E_c \cup E_h$,

(i) if condition $(R_1)$ holds for all $0 \leq n \leq N_*$, all roots of Eq (2.10) have negative parts for all $\sigma \geq 0$, then the positive equilibrium $E_*$ of system (1.2) is asymptotically stable;

(ii) if condition $(R_2)$ or $(R_3)$ holds for some $0 \leq n \leq N_*$, all roots of Eq (2.10) have negative parts for $\sigma \in [0, \sigma_*)$, then the positive equilibrium $E_*$ of system (1.2) is asymptotically stable for $\sigma \in [0, \sigma_*)$ and unstable for $\sigma \in (\sigma_*, +\infty)$. Further, if $L'\left(z_{n,k}\right) \neq 0$, then the positive equilibrium $E_*$ of system (1.2) undergoes Hopf bifurcation at $\sigma = \sigma_{n,k}^{(j)}$.

(II) When $(d_{21},\tau) \in E_s^+$, Eq (2.10) has infinitely many positive real roots for all $\sigma \geq 0$, then the positive equilibrium $E_*$ of system (1.2) is always unstable.

(III) When $d_{21} < d_S^*$,

(i) if condition $(R_1)$ holds for all $0 \leq n \leq N_*$, Eq (2.10) only has one zero root at $\tau = \tau_S$ for all $\sigma \geq 0$, and all other roots of Eq (2.10) have negative parts, then the positive equilibrium $E_*$ of system (1.2) undergoes Turing bifurcation at $\tau = \tau_S$ for all $\sigma \geq 0$;

(ii) if condition $(R_2)$ or $(R_3)$ holds for some $0 \le n \le N_*$, Eq (2.10) has a zero root and a pair of purely imaginary roots at $(\tau, \sigma) = \left(\tau_S, \sigma_{n,k}^{(j)}\right)$ for $0 \le n \le N_*, k = 1, 2, 3, j \in \mathbb{N}_0$, then the positive equilibrium $E_*$ of system (1.2) undergoes Turing–Hopf bifurcation at $(\tau, \sigma) = \left(\tau_S, \sigma_{n,k}^{(j)}\right)$.

## 3. Direction and stability of Hopf bifurcation

From Theorem 2.9, we know that system (1.2) undergoes Hopf bifurcation at $\tau = \tau_n^{\pm}$ for $d_{21} > d_H^*$ and $n \in S_H(d_{21})$ when $\sigma = 0$. From [29], system (1.2) with $\sigma = 0$ is equivalent to the following system:

$$\begin{cases} \dfrac{\partial u(x,t)}{\partial t} = d_{11}\Delta u(x,t) + \dfrac{ru(x,t)}{1+kv(x,t)} - r_0 u(x,t) - r_1 u^2(x,t) - \dfrac{au^2(x,t)v(x,t)}{bu^2(x,t)+u(x,t)+c}, & 0 < x < l\pi, t > 0, \\ \dfrac{\partial v(x,t)}{\partial t} = d_{22}\Delta v(x,t) - d_{21}\left[v(x,t)w_x(x,t)\right]_x - mv(x,t) \\ \qquad\qquad + \dfrac{\eta a u^2(x,t)v(x,t)}{bu^2(x,t)+u(x,t)+c}\left(\dfrac{v(x,t)}{v(x,t)+\theta}\right), & 0 < x < l\pi, t > 0, \\ \dfrac{\partial w(x,t)}{\partial t} = d_{22}\Delta w(x,t) + \dfrac{1}{\tau}(u(x,t) - w(x,t)), & 0 < x < l\pi, t > 0, \\ u_x(x,t) = v_x(x,t) = w_x(x,t) = 0, & x = 0, l\pi, t > 0. \end{cases} \tag{3.1}$$

In this section, we analyze the direction and stability of Hopf bifurcations through the application of normal form theory at $\tau = \tau_n^{\pm}$ for $d_{21} > d_H^*$ and $n \in S_H(d_{21})$. Let $\tau_H$ (where $\tau_H = \tau_{n_H}^+$ or $\tau_H = \tau_{n_H}^-$) denote the critical delay parameter value corresponding to the mode-$n_H$ Hopf bifurcation, with some $n = n_H \in \mathbb{N}$. According to Theorem 2.9, when $\tau = \tau_H$, the characteristic equation (2.12) possesses a pair of purely imaginary eigenvalues $\pm i\varpi_{n_H}$ $(\varpi_{n_H} > 0)$. Define the real-valued Sobolev space

$$\mathscr{X} = \left\{ U = (u, v, w)^T \in \left(W^{2,2}(0, \ell\pi)\right)^3, \frac{\partial u}{\partial x} = \frac{\partial v}{\partial x} = \frac{\partial w}{\partial x} = 0, x = 0, \ell\pi \right\},$$

with the inner product

$$[U, V] = \int_0^{\ell\pi} U^T V dx, \text{ for } U, V \in \mathscr{X}.$$

It is well known that the eigenvalue problem (2.4) has eigenvalues $(\frac{n}{l})^2, n \in \mathbb{N}_0$ with the corresponding normalized eigenfunctions

$$b_n(x) = \frac{\cos\left(\frac{nx}{l}\right)}{\left\|\cos\left(\frac{nx}{l}\right)\right\|_{L^2}} = \begin{cases} \frac{1}{\sqrt{l\pi}}, & \text{when} \quad n = 0, \\ \sqrt{\frac{2}{l\pi}}\cos\left(\frac{nx}{l}\right), & \text{when} \quad n \neq 0. \end{cases}$$

Take the vector $\beta_n^{(1)} = (b_n, 0, 0)^T$, $\beta_n^{(2)} = (0, b_n, 0)^T$, $\beta_n^{(3)} = (0, 0, b_n)^T$. Then we take a small perturbation of $\tau_H$ by setting $\tau = \tau_H + \mu$, $|\mu| \ll 1$ such that $\mu = 0$ corresponds to the Hopf bifurcation value for system (3.1). Also, let

$$\mathfrak{B}(\alpha\omega_1^{r_1}\omega_2^{r_2}\mu^{r_3}) = \begin{pmatrix} \alpha\omega_1^{r_1}\omega_2^{r_2}\mu^{r_3} \\ \overline{\alpha}\omega_1^{r_2}\omega_2^{r_1}\mu^{r_3} \end{pmatrix}, \alpha \in \mathbb{C}.$$

Now, transfer $E_*$ to the origin by setting

$$(\tilde{u}(x,t), \tilde{v}(x,t), \tilde{w}(x,t))^T = (u(x,t), v(x,t), w(x,t))^T - (u_*, v_*, u_*)^T.$$

Let $U = (u, v, w)^T$. Then model (3.1) can be rewritten as the following form:

$$\frac{dU}{dt} = \delta\Delta U + L(\mu)(U) + F(U), \tag{3.2}$$

where $\delta\Delta U = \delta_0\Delta U + F^d(U)$, $L(\mu)(U) = L_0(U) + \tilde{L}(U, \mu)$, and

$$F(U) = \begin{pmatrix} f(u+u_*, v+v_*) \\ g(u+u_*, v+v_*) \\ \frac{1}{\tau_H}(u-w) \end{pmatrix} - L_0(U), \delta_0 = \begin{pmatrix} d_{11} & 0 & 0 \\ 0 & d_{22} & -d_{21}v_* \\ 0 & 0 & d_{22} \end{pmatrix}, \tag{3.3}$$

$$\delta_0\Delta U = -\frac{n^2}{l^2}\begin{pmatrix} d_{11} & 0 & 0 \\ 0 & d_{22} & -d_{21}v_* \\ 0 & 0 & d_{22} \end{pmatrix}\begin{pmatrix} u \\ v \\ w \end{pmatrix}, F^d(U) = -d_{21}\begin{pmatrix} 0 \\ v_x w_x + v w_{xx} \\ 0 \end{pmatrix}, \tag{3.4}$$

and

$$L_0 = \begin{pmatrix} \alpha_{11} & \alpha_{12} & 0 \\ \beta_{21} & \alpha_1 + \alpha_2 & 0 \\ \frac{1}{\tau_H} & 0 & -\frac{1}{\tau_H} \end{pmatrix}, \widetilde{L}(U, \mu) = \begin{pmatrix} 0 \\ 0 \\ \left(\tau_H(\mu) - \frac{1}{\tau_H}\right)(u-w) \end{pmatrix}. \tag{3.5}$$

We denote $\tau_H(\mu) = \frac{1}{\tau_H + \mu}$ in (3.5), and it can be written as a Taylor expansion as follows:

$$\tau_H(\mu) = \frac{1}{\tau_H + \mu} = \sum_{j=1}^{\infty}(-1)^{j-1}\frac{1}{\tau_H^j}\mu^{j-1}.$$

In the subsequent analysis, we assume that the functional $F(U)$ possesses $C^k$ smoothness with respect to the delay variable $U$, where $k \geq 3$. Given that the perturbation parameter $\mu$ is treated as an independent variable in the normal form computation, we reformulate Eq (3.2) into the following extended system:

$$\frac{dU}{dt} = \delta_0\Delta U + L_0(U) + \widetilde{F}(U, \mu), \tag{3.6}$$

where

$$\widetilde{F}(U, \mu) = F(U) + \widetilde{L}(U, \mu) + F^d(U). \tag{3.7}$$

Denoting by $\mathscr{L}(U) = \delta_0\Delta U + L_0(U)$, the linear system of Eq (3.6) can be written as

$$\frac{dU}{dt} = \mathscr{L}(U). \tag{3.8}$$

Let $\Lambda = \{i\varpi_{n_H}, -i\varpi_{n_H}\}$, and denote the generalized eigenspace of Eq (3.8) associated with $\Lambda$ by $\Phi$ and the corresponding adjoint space by $\Phi^*$. Then, according to the standard adjoint theory for ODEs, $\mathbb{C}^3$ can be decomposed by $\Lambda$ as $\mathbb{C}^3 = \Phi \oplus \Psi$, where $\Psi = \left\{\psi \in \mathbb{C}^3 : \langle\varphi, \psi\rangle = 0, \forall\varphi \in \Phi^*\right\}$ and $\langle\cdot,\cdot\rangle$ is defined by $\langle\varphi, \psi\rangle = \varphi^T\psi$, for $\varphi, \psi \in \mathbb{C}^3$.

Let $\mathcal{P} = (p, \overline{p}), \mathcal{Q} = (q^{\mathrm{T}}, \overline{q}^{\mathrm{T}})^{\mathrm{T}}$, where $p = (p_1, p_2, p_3)^{\mathrm{T}}$ and $q = (q_1, q_2, q_3)^{\mathrm{T}}$. Choose the dual bases $\mathcal{P}$ and $\mathcal{Q}$ of $\Phi$ and $\Phi^*$ such that

$$\langle\mathcal{Q}, \mathcal{P}\rangle = E_2.$$

Through algebraic reduction, we get

$$p = \begin{pmatrix} 1 \\ \frac{i\varpi_{n_H} - \alpha_{11} + d_{11}(\frac{n_H}{l})^2}{\alpha_{12}} \\ \frac{1}{k_1} \end{pmatrix} \text{ and } q = \eta \begin{pmatrix} 1 \\ \frac{\alpha_{12}}{k_2} \\ \frac{\tau_H d_{21}\alpha_{12}(\frac{n_H}{l})^2 v_*}{k_1 k_2} \end{pmatrix}.$$

Here,

$$\eta = \frac{k_1^2 k_2}{k_1^2\left(2i\varpi_{n_H} + (d_{11}+d_{22})(\frac{n_H}{l})^2 - (\alpha_{11}+\alpha_1+\alpha_2)\right) + \tau_H d_{21}\alpha_{12}v_*(\frac{n_H}{l})^2},$$

with $k_1 = d_{22}\tau_H\left(\frac{n_H}{l}\right)^2 + 1 + i\varpi_{n_H}\tau_H$ and $k_2 = d_{22}\left(\frac{n_H}{l}\right)^2 - \alpha_1 - \alpha_2 + i\varpi_{n_H}$.

Furthermore, from $\mathbb{C}^3 = \Phi \oplus \Psi$, we see that $\mathscr{X}$ can be decomposed as

$$\mathscr{X} = Im\pi \oplus Ker\pi,$$

where $dim\ Im\pi = 2$, for $\tilde{\psi} \in \mathscr{X}$, the projection $\pi : \mathscr{X} \to Im\pi$ is defined by

$$\pi(\tilde{\psi}) = \left(\mathcal{P}\left\langle \mathcal{Q}, \begin{pmatrix} [\widetilde{\psi}(\cdot), \beta_{n_H}^{(1)}] \\ [\widetilde{\psi}(\cdot), \beta_{n_H}^{(2)}] \\ [\widetilde{\psi}(\cdot), \beta_{n_H}^{(3)}] \end{pmatrix} \right\rangle\right)^{\mathrm{T}} b_{n_H}(x). \tag{3.9}$$

Hence, we can decompose $U$ as

$$U = \mathcal{P}\omega b_{n_H}(x) + z, \quad z = (z^{(1)}, z^{(2)}, z^{(3)})^T \in Ker\pi,$$

where $\omega = (\omega_1(t), \omega_2(t)) \in \mathbb{R}^2$. Consequently, we decompose system (3.6) as the following equations:

$$\begin{cases} \dot{\omega} = \mathfrak{D}\omega + \mathcal{Q}\begin{pmatrix} [\tilde{F}(\mathcal{P}\omega b_{n_H}(x) + z, \mu), \beta_{n_H}^{(1)}] \\ [\tilde{F}(\mathcal{P}\omega b_{n_H}(x) + z, \mu), \beta_{n_H}^{(2)}] \\ [\tilde{F}(\mathcal{P}\omega b_{n_H}(x) + z, \mu), \beta_{n_H}^{(3)}] \end{pmatrix}, \\ \dot{z} = \mathscr{L}(z) + (I - \pi)\tilde{F}(\mathcal{P}\omega b_{n_H}(x) + z, \mu), \end{cases} \tag{3.10}$$

where $\mathfrak{D} = \mathrm{diag}\{i\varpi_{n_H}, -i\varpi_{n_H}\}$.

Now, we consider the following Taylor expansion:

$$\widetilde{F}(\psi, \mu) = \sum_{j\geq 2}\frac{1}{j!}\widetilde{F}_j(\psi, \mu), F(\psi) = \sum_{j\geq 2}\frac{1}{j!}F_j(\psi),$$
$$\widetilde{L}(\psi, \mu) = \sum_{j\geq 1}\frac{1}{j!}\widetilde{L}_j(\psi)\mu^j, F^d(\psi) = \sum_{j\geq 2}\frac{1}{j!}F_j^d(\psi),$$

we have

$$\widetilde{F}_j(\psi, \mu) = F_j(\psi) + j\mu^{j-1}\widetilde{L}_{j-1}(\psi) + F_j^d(\psi), \quad j = 2, 3\cdots. \tag{3.11}$$

The system (3.10) can be rewritten as

$$\begin{cases} \dot{\omega} = \mathfrak{D}\omega + \sum_{j\geq 2}\frac{1}{j!}f_j^1(\omega, z, \mu), \\ \dot{z} = \mathscr{L}(z) + \sum_{j\geq 2}\frac{1}{j!}f_j^2(\omega, z, \mu), \end{cases} \tag{3.12}$$

where

$$\begin{cases} f_j^1(\omega,z,\mu) = Q\begin{pmatrix}[\tilde{F}_j(\mathcal{P}\omega b_{n_H}(x)+z,\mu),\beta_{n_H}^{(1)}]\\ [\tilde{F}_j(\mathcal{P}\omega b_{n_H}(x)+z,\mu),\beta_{n_H}^{(2)}]\\ [\tilde{F}_j(\mathcal{P}\omega b_{n_H}(x)+z,\mu),\beta_{n_H}^{(3)}]\end{pmatrix},\\ f_j^2(\omega,z,\mu) = (I-\pi)\tilde{F}_j(\mathcal{P}\omega b_{n_H}(x)+z,\mu). \end{cases} \tag{3.13}$$

By implementing the subsequent change of variables [26],

$$(\omega,z) = (\tilde{\omega},\tilde{z}) + \frac{1}{j!}\left(U_j^1(\tilde{\omega},\mu), U_j^2(\tilde{\omega},\mu)\right), j \geq 2, \tag{3.14}$$

we thereby derive the normal form of system (3.12) as follows:

$$\dot{\omega} = \mathfrak{D}\omega + \sum_{j\geq 2}\frac{1}{j!}g_j^1(\omega,0,\mu). \tag{3.15}$$

Define the operators $(M_j^1 p)(\omega,\mu) = D_\omega p(\omega,\mu)\mathfrak{D}\omega - \mathfrak{D}p(\omega,\mu)$ and $(M_j^2 h)(\omega,\mu) = D_\omega h(\omega,\mu)\mathfrak{D}\omega - \mathscr{L}(h(\omega,\mu))$. Applying the method from [26, 30], we compute

$$g_2^1(\omega,0,\mu) = \mathrm{Proj}_{\ker(M_2^1)} f_2^1(\omega,0,\mu),$$

and

$$g_3^1(\omega,0,\mu) = \mathrm{Proj}_{\ker(M_3^1)}\tilde{f}_3^1(\omega,0,\mu) = \mathrm{Proj}_S\tilde{f}_3^1(\omega,0,0) + O(\mu^2|\omega|). \tag{3.16}$$

Here, the cubic polynomial is interpreted in the coordinate system induced by transformation (3.14). Furthermore, it can be determined by (3.16) that

$$\ker(M_2^1) = \mathrm{Span}\left\{\begin{pmatrix}\mu\omega_1\\0\end{pmatrix},\begin{pmatrix}0\\\mu\omega_2\end{pmatrix}\right\},$$
$$\ker(M_3^1) = \mathrm{Span}\left\{\begin{pmatrix}\omega_1^2\omega_2\\0\end{pmatrix},\begin{pmatrix}\mu^2\omega_1\\0\end{pmatrix},\begin{pmatrix}0\\\omega_1\omega_2^2\end{pmatrix},\begin{pmatrix}0\\\mu^2\omega_2\end{pmatrix}\right\},$$

and

$$S = \mathrm{Span}\left\{\begin{pmatrix}\omega_1^2\omega_2\\0\end{pmatrix},\begin{pmatrix}0\\\omega_1\omega_2^2\end{pmatrix}\right\}. \tag{3.17}$$

### *3.1. Calculation of $g_2^1(\omega,0,\xi)$*

From (3.11), we get

$$\widetilde{F}_2(\psi,\mu) = F_2(\psi) + 2\mu\widetilde{L}_1(\psi) + F_2^d(\psi).$$

From (3.4), we have

$$F_2^d(U) = -2d_{21}(0, v_x w_x + v w_{xx}, 0)^T, F_j^d(U) = (0,0,0)^T, j = 3,4,\cdots, \tag{3.18}$$

and from (3.5) and (3.11), we obtain

$$\widetilde{L}_j(U) = \left(0,0,(-1)^j\frac{1}{\tau_H^{j+1}}(u-w)\right)^T, j \geq 1. \tag{3.19}$$

Clearly, because for $n \in \mathbb{N}$, $\int_0^{l\pi} b_n^2(x)dx = 1$, we can calculate that

$$\begin{pmatrix} \begin{bmatrix} 2\mu\tilde{L}_1\left(\mathcal{P}\omega b_{n_H}(x)\right), \beta_{n_H}^{(1)} \end{bmatrix} \\ \begin{bmatrix} 2\mu\tilde{L}_1\left(\mathcal{P}\omega b_{n_H}(x)\right), \beta_{n_H}^{(2)} \end{bmatrix} \\ \begin{bmatrix} 2\mu\tilde{L}_1\left(\mathcal{P}\omega b_{n_H}(x)\right), \beta_{n_H}^{(3)} \end{bmatrix} \end{pmatrix} = -\frac{2\mu}{\tau_H^2} \begin{pmatrix} 0 \\ 0 \\ (p_1 - p_3)\,\omega_1 + (\overline{p}_1 - \overline{p}_3)\,\omega_2 \end{pmatrix}. \tag{3.20}$$

From (3.3) and (3.4), we obtain that $F_2(\psi)$ and $F_2^d(\psi)$ do not contain the variable $\mu$. It follows from the first mathematical expression in (3.13) that

$$f_2^1(\omega, 0, \mu) = Q \begin{pmatrix} [\tilde{F}_2(\mathcal{P}\omega b_{n_H}(x), \mu), \beta_{n_H}^{(1)}] \\ [\tilde{F}_2(\mathcal{P}\omega b_{n_H}(x), \mu), \beta_{n_H}^{(2)}] \\ [\tilde{F}_2(\mathcal{P}\omega b_{n_H}(x), \mu), \beta_{n_H}^{(3)}] \end{pmatrix}.$$

This, together with (3.11), (3.18), and (3.19), leads to

$$g_2^1(\omega, 0, \mu) = \mathrm{Proj}_{\ker(M_2^1)} f_2^1(\omega, 0, \mu) = \mathfrak{B}(B_1\mu\omega_1), \tag{3.21}$$

where

$$B_1 = -\frac{2}{\tau_H^2} q_3(p_1 - p_3). \tag{3.22}$$

### *3.2. Calculation of* $g_3^1(\omega, 0, \xi)$

Similar to [31], denote

$$f_2^{(1,1)}(\omega, z, 0) = Q \begin{pmatrix} [F_2(\mathcal{P}\omega b_{n_H}(x) + z), \beta_{n_H}^{(1)}] \\ [F_2(\mathcal{P}\omega b_{n_H}(x) + z), \beta_{n_H}^{(2)}] \\ [F_2(\mathcal{P}\omega b_{n_H}(x) + z), \beta_{n_H}^{(3)}] \end{pmatrix}, \tag{3.23}$$

and

$$f_2^{(1,2)}(\omega, z, 0) = Q \begin{pmatrix} [F_2^d(\mathcal{P}\omega b_{n_H}(x) + z), \beta_{n_H}^{(1)}] \\ [F_2^d(\mathcal{P}\omega b_{n_H}(x) + z), \beta_{n_H}^{(2)}] \\ [F_2^d(\mathcal{P}\omega b_{n_H}(x) + z), \beta_{n_H}^{(3)}] \end{pmatrix}. \tag{3.24}$$

(3.21) implies that $g_2^1(\omega, 0, 0) = (0, 0)^T$. Then $\tilde{f}_3^1(\omega, 0, 0)$ is determined by

$$\begin{aligned} \tilde{f}_3^1(\omega, 0, 0) =& f_3^1(\omega, 0, 0) + \frac{3}{2}\Big[\Big(D_\omega f_2^1(\omega, 0, 0)\Big)U_2^1(\omega, 0) \\ &+ \Big(D_z f_2^{(1,1)}(\omega, 0, 0)\Big)U_2^2(\omega, 0) + \\ &\Big(D_{z,z_x,z_{xx}} f_2^{(1,2)}(\omega, 0, 0)\Big)U_2^{(2,d)}(\omega, 0)\Big], \end{aligned}$$

where $f_2^1(\omega, 0, 0) = f_2^{(1,1)}(\omega, 0, 0) + f_2^{(1,2)}(\omega, 0, 0)$,

$$\begin{aligned} &D_{z,z_x,z_{xx}} f_2^{(1,2)}(\omega, 0, 0) = \Big(D_z f_2^{(1,2)}(\omega, 0, 0), D_{z_x} f_2^{(1,2)}(\omega, 0, 0), D_{z_{xx}} f_2^{(1,2)}(\omega, 0, 0)\Big), \\ &U_2^1(\omega, 0) = (M_2^1)^{-1}\mathrm{Proj}_{Im(M_2^1)} f_2^1(\omega, 0, 0), U_2^2(\omega, 0) = (M_2^2)^{-1} f_2^2(\omega, 0, 0), \end{aligned} \tag{3.25}$$

and

$$U_2^{(2,d)}(\omega,0)=\left(U_2^2(\omega,0),U_{2x}^2(\omega,0),U_{2xx}^2(\omega,0)\right)^{\mathrm{T}}. \tag{3.26}$$

We next finish the calculation of $\mathrm{Proj}_S\ \tilde{f}_3^1(\omega,0,0)$ in four steps.

**Step 1**. The calculation of $\mathrm{Proj}_S\ f_3^1(\omega,0,0)$

Wring $F_3(\mathcal{P}\omega b_{n_H}(x))$ as follows:

$$F_3(\mathcal{P}\omega b_{n_H}(x))=\sum_{r_1+r_2=3}\mathcal{A}_{r_1r_2}\omega_1^{r_1}\omega_2^{r_2}b_{n_H}^3(x),r_1,r_2\in\mathbb{N}_0, \tag{3.27}$$

where $\mathcal{A}_{r_1r_2}=\overline{\mathcal{A}}_{r_2r_1}$ with $r_1,r_2\in\mathbb{N}_0$. From (3.7), (3.18), and (3.19), we have $\tilde{F}_3(\mathcal{P}\omega b_{n_H}(x),0)=F_3(\mathcal{P}\omega b_{n_H}(x))$. From (3.13) and (3.27), we deduce

$$f_3^1(\omega,0,0)=Q\left(\sum_{r_1+r_2=3}\mathcal{A}_{r_1r_2}\omega_1^{r_1}\omega_2^{r_2}\int_0^{l\pi}b_{n_H}^4(x)\mathrm{d}x\right),$$

which, together with $\int_0^{l\pi}b_{n_H}^4(x)\mathrm{d}x=\frac{3}{2l\pi}$, yields

$$\mathrm{Proj}_S f_3^1(\omega,0,0)=\mathfrak{B}(B_{21}\omega_1^2\omega_2),$$

where

$$B_{21}=\frac{3}{2l\pi}q^{\mathrm{T}}\mathcal{A}_{21}.$$

**Step 2**. The calculation of $\mathrm{Proj}_S((D_\omega f_2^1(\omega,0,0))U_2^1(\omega,0))$

From (3.7), (3.18), and (3.19), we have that

$$\tilde{F}_2(\mathcal{P}\omega b_{n_H}(x),0)=F_2(\mathcal{P}\omega b_{n_H}(x))+F_2^d(\mathcal{P}\omega b_{n_H}(x)). \tag{3.28}$$

(3.27) implies

$$F_2(\mathcal{P}\omega b_{n_H}(x)+z)=b_{n_H}^2(x)\left(\sum_{r_1+r_2=2}\mathcal{A}_{r_1r_2}\omega_1^{r_1}\omega_2^{r_2}\right)+S_2(\mathcal{P}\omega b_{n_H}(x),z)+O(|z|^2), \tag{3.29}$$

where $S_2(\mathcal{P}\omega b_{n_H}(x),z)$ refers to the product of $\mathcal{P}\omega b_{n_H}(x)$ and $z$. In conjunction with (3.18), we write

$$F_2^d(\mathcal{P}\omega b_{n_H}(x))=\left(\frac{n_H}{l}\right)^2\left(\xi_{n_H}^2(x)-b_{n_H}^2(x)\right)\left(\sum_{r_1+r_2=2}\mathcal{A}_{r_1r_2}^d\omega_1^{r_1}\omega_2^{r_2}\right), \tag{3.30}$$

where

$$\xi_{n_H}(x)=\sqrt{\frac{2}{l\pi}}\sin\left(\frac{n_Hx}{l}\right),$$

and

$$\mathcal{A}_{20}^d=-2d_{21}\begin{pmatrix}0\\p_2p_3\\0\end{pmatrix}=\overline{\mathcal{A}_{02}^d},\mathcal{A}_{11}^d=-4d_{21}\begin{pmatrix}0\\\mathrm{Re}\{p_2\bar{p}_3\}\\0\end{pmatrix}. \tag{3.31}$$

It then follows from $\int_0^{l\pi} \xi_{n_H}^2(x) b_{n_H}(x)\mathrm{d}x = \int_0^{l\pi} b_{n_H}^3(x)\mathrm{d}x = 0$ that

$$f_2^1(\omega,0,0) = \mathcal{Q}\begin{pmatrix}[\tilde{F}_2(\mathcal{P}\omega b_{n_H}(x),0),\beta_{n_H}^{(1)}]\\ [\tilde{F}_2(\mathcal{P}\omega b_{n_H}(x),0),\beta_{n_H}^{(2)}]\\ [\tilde{F}_2(\mathcal{P}\omega b_{n_H}(x),0),\beta_{n_H}^{(3)}]\end{pmatrix} = (0,0,0)^{\mathrm{T}}. \tag{3.32}$$

Hence, together with (3.27), (3.29), and (3.30), we have

$$\mathrm{Proj}_S\left((D_\omega f_2^1(\omega,0,0))U_2^1(\omega,0)\right) = \mathfrak{B}(B_{22}\omega_1^2\omega_2),$$

where

$$B_{22} = (0,0)^{\mathrm{T}}, n_H \in \mathbb{N}.$$

**Step 3**. The calculation of $\mathrm{Proj}_S\left((D_z f_2^{(1,1)}(\omega,0,0))U_2^2(\omega,0)\right)$

Denote

$$U_2^2(\omega,0) = h(\omega) = \sum_{n\in\mathbb{N}_0} h_n(\omega)b_n(x) \in Ker\pi,$$

where $h_n(\omega) = \sum_{r_1+r_2=2} h_{n,r_1r_2}\omega_1^{r_1}\omega_2^{r_2}$. We can derive from [31] that

$$\begin{pmatrix}[S_2(\mathcal{P}\omega b_{n_H}(x),\sum_{n\in\mathbb{N}_0} h_n(\omega)b_n(x)),\beta_{n_H}^{(1)}]\\ [S_2(\mathcal{P}\omega b_{n_H}(x),\sum_{n\in\mathbb{N}_0} h_n(\omega)b_n(x)),\beta_{n_H}^{(2)}]\\ [S_2(\mathcal{P}\omega b_{n_H}(x),\sum_{n\in\mathbb{N}_0} h_n(\omega)b_n(x)),\beta_{n_H}^{(3)}]\end{pmatrix} = \sum_{n\in\mathbb{N}_0} H_n\left(S_2(p\omega_1,h_n(\omega)) + S_2(\bar{p}\omega_2,h_n(\omega))\right),$$

where

$$H_n = \int_0^{l\pi} b_{n_H}^2(x)b_n(x)\mathrm{d}x = \begin{cases}\frac{1}{\sqrt{l\pi}}, & n=0,\\ \frac{1}{\sqrt{2l\pi}}, & n=2n_H,\\ 0, & \text{otherwise.}\end{cases}$$

Hence, we have

$$(D_z f_2^{(1,1)}(\omega,0,0))U_2^2(\omega,0) = \mathcal{Q}\left(\sum_{n=0,n=2n_H} H_n\left(S_2(p\omega_1,h_n(\omega)) + S_2(\bar{p}\omega_2,h_n(\omega))\right)\right),$$

and

$$\mathrm{Proj}_S((D_z f_2^{(1,1)}(\omega,0,0))U_2^2(\omega,0)) = \mathfrak{B}(B_{23}\omega_1^2\omega_2),$$

where

$$B_{23} = \frac{1}{\sqrt{l\pi}}q^{\mathrm{T}}\left(S_2(p,h_{0,11}) + S_2(\bar{p},h_{0,20})\right) + \frac{1}{\sqrt{2l\pi}}q^{\mathrm{T}}\left(S_2(p,h_{2n_H,11}) + S_2(\bar{p},h_{2n_H,20})\right).$$

**Step 4**. The calculation of $\mathrm{Proj}_S\left((D_{z,z_x,z_{xx}} f_2^{(1,2)}(\omega,0,0))U_2^{(2,d)}(\omega,0)\right)$

Let $U = (U^{(1)},U^{(2)},U^{(3)}) = \mathcal{P}\omega b_{n_H}(x)$ and

$$\begin{aligned}F_2^d(\mathcal{P}\omega b_{n_H}(x),z,z_x,z_{xx}) &= F_2^d(\mathcal{P}\omega b_{n_H}(x)+z,0)\\ &= -2d_{21}\begin{pmatrix}0\\ (U_x^{(2)}+z_x^{(2)})(U_x^{(3)}+z_x^{(3)})\\ 0\end{pmatrix} - 2d_{21}\begin{pmatrix}0\\ (U^{(2)}+z^{(2)})(U_{xx}^{(3)}+z_{xx}^{(3)})\\ 0\end{pmatrix},\end{aligned}$$

$$\begin{cases} S_2^{(d,1)}(U,z) = -2d_{21}\begin{pmatrix} 0 \\ U_{xx}^{(3)} z^{(2)} \\ 0 \end{pmatrix}, \\ S_2^{(d,2)}(U,z_x) = -2d_{21}\begin{pmatrix} 0 \\ U_x^{(2)} z_x^{(3)} \\ 0 \end{pmatrix} - 2d_{21}\begin{pmatrix} 0 \\ U_x^{(3)} z_x^{(2)} \\ 0 \end{pmatrix}, \\ S_2^{(d,3)}(U,z_{xx}) = -2d_{21}\begin{pmatrix} 0 \\ U^{(2)} z_{xx}^{(3)} \\ 0 \end{pmatrix}. \end{cases}$$

Because

$$\begin{aligned} U_2^2(\omega,0) = h(\omega) &= \sum_{n\in\mathbb{N}_0} h_n(\omega) b_n(x), \\ U_{2x}^2(\omega,0) = h_x(\omega) &= -\sum_{n\in\mathbb{N}_0} \left(\frac{n}{l}\right) h_n(\omega)\xi_n(x), \\ U_{2xx}^2(\omega,0) = h_{xx}(\omega) &= -\sum_{n\in\mathbb{N}_0} \left(\frac{n}{l}\right)^2 h_n(\omega) b_n(x), \end{aligned}$$

then we get

$$\begin{aligned} &D_{z,z_x,z_{xx}} F_2^d\left(\mathcal{P}\omega b_{n_H}(x), z, z_x, z_{xx}\right) U_2^{(2,d)}(\omega,0) \\ =&S_2^{(d,1)}(\mathcal{P}\omega b_{n_H}(x), h(\omega)) + S_2^{(d,2)}\left(\mathcal{P}\omega b_{n_H}(x), h_x(\omega)\right) + S_2^{(d,3)}\left(\mathcal{P}\omega b_{n_H}(x), h_{xx}(\omega)\right), \end{aligned}$$

and

$$\left(\begin{bmatrix} S_2^{(d,1)}\left(\mathcal{P}\omega b_{n_H}(x), h(\omega)\right), \beta_{n_H}^{(1)}(x) \\ S_2^{(d,1)}\left(\mathcal{P}\omega b_{n_H}(x), h(\omega)\right), \beta_{n_H}^{(2)}(x) \\ S_2^{(d,1)}\left(\mathcal{P}\omega b_{n_H}(x), h(\omega)\right), \beta_{n_H}^{(3)}(x) \end{bmatrix}\right) = -\left(\frac{n_H}{l}\right)^2 \sum_{n\in\mathbb{N}_0} H_n\left(\tilde{S}_2^{(d,1)}\left(p\omega_1, h_n(\omega)\right) + \tilde{S}_2^{(d,1)}\left(\bar{p}\omega_2, h_n(\omega)\right)\right),$$

$$\left(\begin{bmatrix} S_2^{(d,2)}\left(\mathcal{P}\omega b_{n_H}(x), h_x(\omega)\right), \beta_{n_H}^{(1)}(x) \\ S_2^{(d,2)}\left(\mathcal{P}\omega b_{n_H}(x), h_x(\omega)\right), \beta_{n_H}^{(2)}(x) \\ S_2^{(d,2)}\left(\mathcal{P}\omega b_{n_H}(x), h_x(\omega)\right), \beta_{n_H}^{(3)}(x) \end{bmatrix}\right) = \left(\frac{n_H}{l}\right) \sum_{n\in\mathbb{N}_0} \left(\frac{n}{l}\right) C_n\left(\tilde{S}_2^{(d,2)}\left(p\omega_1, h_n(\omega)\right) + \tilde{S}_2^{(d,2)}\left(\bar{p}\omega_2, h_n(\omega)\right)\right),$$

$$\left(\begin{bmatrix} S_2^{(d,3)}\left(\mathcal{P}\omega b_{n_H}(x), h_{xx}(\omega)\right), \beta_{n_H}^{(1)}(x) \\ S_2^{(d,3)}\left(\mathcal{P}\omega b_{n_H}(x), h_{xx}(\omega)\right), \beta_{n_H}^{(2)}(x) \\ S_2^{(d,3)}\left(\mathcal{P}\omega b_{n_H}(x), h_{xx}(\omega)\right), \beta_{n_H}^{(3)}(x) \end{bmatrix}\right) = -\sum_{n\in\mathbb{N}_0} \left(\frac{n}{l}\right)^2 H_n\left(\tilde{S}_2^{(d,3)}\left(p\omega_1, h_n(\omega)\right) + \tilde{S}_2^{(d,3)}\left(\bar{p}\omega_2, h_n(\omega)\right)\right),$$

where

$$C_n = \int_0^{l\pi} \xi_{n_H}(x)\xi_n(x) b_{n_H}(x) dx = \begin{cases} \frac{1}{\sqrt{2l\pi}}, & n = 2n_H, \\ 0, & \text{otherwise}, \end{cases}$$

as well as

$$\widetilde{S}_2^{(d,1)}(p,z) = -2d_{21}\begin{pmatrix} 0 \\ z_2p_3 \\ 0 \end{pmatrix}, \widetilde{S}_2^{(d,2)}(p,z) = -2d_{21}\begin{pmatrix} 0 \\ z_3p_2 + z_2p_3 \\ 0 \end{pmatrix}, \widetilde{S}_2^{(d,3)}(p,z) = -2d_{21}\begin{pmatrix} 0 \\ z_3p_2 \\ 0 \end{pmatrix}.$$

From (3.23)–(3.26), we have

$$\Big(D_{z,z_x,z_{xx}} f_2^{(1,2)}(\omega,0,0)\Big) U_2^{(2,d)}(\omega,0) = Q\begin{pmatrix} \Big[D_{z,z_x,z_{xx}} F_2^d(\mathcal{P}\omega b_{n_H}(x), z, z_x, z_{xx}) U_2^{(2,d)}(\omega,0), \beta_{n_H}^{(1)}\Big] \\ \Big[D_{z,z_x,z_{xx}} F_2^d(\mathcal{P}\omega b_{n_H}(x), z, z_x, z_{xx}) U_2^{(2,d)}(\omega,0), \beta_{n_H}^{(2)}\Big] \\ \Big[D_{z,z_x,z_{xx}} F_2^d(\mathcal{P}\omega b_{n_H}(x), z, z_x, z_{xx}) U_2^{(2,d)}(\omega,0), \beta_{n_H}^{(3)}\Big] \end{pmatrix},$$

and

$$\mathrm{Proj}_S((D_{z,z_x,z_{xx}} f_2^{(1,2)}(\omega,0,0)) U_2^{(2,d)}(\omega,0)) = \mathfrak{B}(B_{24}\omega_1^2\omega_2),$$

where

$$\begin{aligned} B_{24} = &-\frac{1}{\sqrt{l\pi}}(\frac{n_H}{l})^2 q^{\mathrm{T}}\Big(\tilde{S}_2^{(d,1)}(p, h_{0,11}) + \tilde{S}_2^{(d,1)}(\bar{p}, h_{0,20})\Big) \\ &+ \frac{1}{\sqrt{2l\pi}} q^{\mathrm{T}} \sum_{j=1,2,3} h_{2n_H}^{(j)} \Big(\tilde{S}_2^{(d,j)}(p, h_{2n_H,11}) + \tilde{S}_2^{(d,j)}(\bar{p}, h_{2n_H,20})\Big), \end{aligned}$$

with

$$h_{2n_H}^{(1)} = -\frac{n_H^2}{l^2}, h_{2n_H}^{(2)} = 2\frac{n_H^2}{l^2}, h_{2n_H}^{(3)} = -\frac{4n_H^2}{l^2}.$$

According to the above computations, we can obtain the normal form of Hopf bifurcation as follows:

$$\dot{\omega} = \mathfrak{D}\omega + \frac{1}{2}\begin{pmatrix} B_1\omega_1\mu \\ \bar{B}_1\omega_2\mu \end{pmatrix} + \frac{1}{3!}\begin{pmatrix} B_2\omega_1^2\omega_2 \\ \bar{B}_2\omega_1\omega_2^2 \end{pmatrix} + O(|\omega|\mu^2 + |\omega|^4), \tag{3.33}$$

where

$$B_1 = -\frac{2}{\tau_H^2} q_3\Big(p_1 - p_3\Big), \quad B_2 = B_{21} + \frac{3}{2}(B_{22} + B_{23} + B_{24}).$$

Let $\omega_1 = z_1 - iz_2$, $\omega_2 = z_1 + iz_2$, and $z_1 = \varrho cos\gamma$, $z_2 = \varrho sin\gamma$, where $\gamma$ is the azimuthal angle, then Eq (3.33) can be rewritten in the following polar coordinate form:

$$\dot{\varrho} = K_1\mu\varrho + K_2\varrho^3 + O(\mu^2\varrho + |(\mu,\varrho)|^4),$$

where

$$K_1 = \frac{1}{2}Re(B_1), \quad K_2 = \frac{1}{3!}Re(B_2).$$

We further have the following theorem [32]:

**Theorem 3.1**. The Hopf bifurcation is supercritical (subcritical) provided that $K_1K_2 < 0 (> 0)$, and the bifurcating periodic solutions are stable (unstable) if $K_2 < 0 (> 0)$.

In order to obtain $B_2$, we need to calculate $\mathcal{A}_{ij}$, $S_2(\mathcal{P}\omega b_{n_H}(x), z)$, $h_{0,20}$, $h_{0,11}$, $h_{2n_H,20}$, and $h_{2n_H,11}$. The detailed calculation procedures are provided in the Appendix.

## 4. Numerical simulation

In this section, we conduct a series of numerical simulations to validate the preceding theoretical findings. We set the parameters as follows:

$$r = 0.14, r_0 = 0.01, k = 3.5, r_1 = 0.01, a = 0.5, b = 0.5, c = 0.01,$$

$$\eta = 0.4, \theta = 0.03, m = 0.25, l = 4, d_{11} = 0.06, d_{22} = 0.2.$$

It can be verified that $(H_1)$ and $(H_2)$ hold, and there is a positive equilibrium $E_* = (0.9268, 0.3312)$.

### *4.1. The Spatiotemporal distribution when $\sigma = 0$*

From (2.9), we have

$$d^S_{21,4} \approx -0.1791 > d^S_{21,5} \approx -0.1820 > d^S_{21,6} \approx -0.2035 > d^S_{21,3} \approx -0.2135 > \dots.$$

Thus, it follows from (2.15) that $d^*_S = d^S_{21,4} \approx -0.1791$. From (2.13), we can calculate that the Turing bifurcation curves are $\tau = \tau^S_n$ for fixed $d_{21} < d^*_S$.

Similar to Proposition 2.6 in [25], we can calculate that $\mu_* \approx 0.2293$. Together with (2.30) and (2.31), we obtain $\hat{n} = 2$ and $d^*_H = \min_{1\le n\le 2}\left\{d^H_{21,n}\right\}$, where, from (2.23),

$$d^H_{21,2} \approx 0.8006 < d^H_{21,1} \approx 0.9263 < \cdots,$$

which implies that $d^*_H = d^H_{21,2} \approx 0.8006$. From (2.21), we can calculate that the Hopf bifurcation curves are $\tau = \tau^{\pm}_n$ for fixed $d_{21} > d^*_H$.

Further, according to Theorems 2.5 and 2.9, we get that for $\sigma = 0$, when $-0.1791 \approx d^*_S < d_{21} < d^*_H \approx 0.8006$, $E_*$ is locally asymptotically stable for all $\tau \ge 0$; when $d_{21} < d^*_S \approx -0.1791$, $E_*$ is locally asymptotically stable for $\tau > \tau_S$ and unstable for $0 < \tau < \tau_S$, and Turing bifurcations occur at $\tau = \tau^S_n$ for fixed $d_{21} < d^S_{21,n}$; when $d_{21} > d^*_H \approx 0.8006$, $E_*$ is locally asymptotically stable for $\tau \in [0, \tau_*) \cup (\tau^*, +\infty)$, and unstable for $\tau \in (\tau_*, \tau^*)$, and Hopf bifurcations occur at $\tau = \tau^{\pm}_n$ for fixed $d_{21} > d^H_{21,n}$ (see Figure 1).

#### 4.1.1. $d_{21} = -0.55 < d^*_S$

For fixed $d_{21} = -0.55 < d^*_S$, it follows from (2.15) that $\tau_S = \tau^S_3 \approx 14.0143$ and $E_*$ is asymptotically stable for $(\tau_S, \infty)$. For $\tau = 14.1 > \tau_S$, $E_*$ is spatially homogeneous steady state (see Figure 2(a),(c)). For $\tau = 13.75 < \tau_S$, $E_*$ is the mode-3 spatially nonhomogeneous steady state (see Figure 2(b),(d)).

#### 4.1.2. $d_{21} = 1.5 > d^*_H$

For fixed $d_{21} = 1.5 > d^*_H$, it follows from (2.33) that

$$\tau_* = \tau^+_2 \approx 1.3313, \tau^* = \tau^-_2 \approx 27.1474.$$

System (1.2) undergoes Hopf bifurcations at $\tau = \tau_*$ and $\tau = \tau^*$, and $E_*$ is asymptotically stable for $\tau \in [0, \tau_*) \cup (\tau^*, \infty)$. Using the procedure developed in Section 3, we have, for $\tau_H = \tau_* \approx 1.3313$,

$$\kappa_1 \approx 0.0418 > 0, \kappa_2 \approx -0.0079 < 0,$$

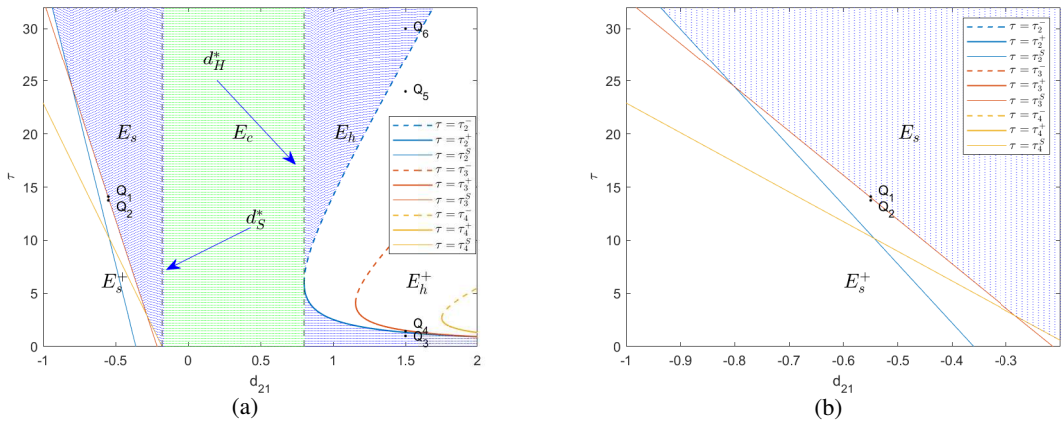


(a) (b)

**Figure 1.** (a) Stability regions and bifurcation curves for system (1.2) with $\sigma = 0$. The areas with blue dots are $E_s$ and $E_h$, and the area with green dots is $E_c$. In the remaining colorless areas, the left side is $E_s^+$, and the right side is $E_h^+$. The Hopf bifurcation curves are $\tau = \tau_n^{\pm}, n = 2, 3, 4$, and the Turing bifurcation curves are $\tau = \tau_n^S, n = 2, 3, 4$. When $(d_{21}, \tau) \in E_s \cup E_c \cup E_h$, $E_*$ is stable for $\sigma = 0$; when $(d_{21}, \tau) \in E_s^+$, $E_*$ is unstable for $\sigma \geq 0$; when $(d_{21}, \tau) \in E_h^+$, $E_*$ is unstable for $\sigma = 0$. (b) is the enlargement of (a) restricted to the region $-1 < d_{21} < -0.2, 0 < \tau < 32$.

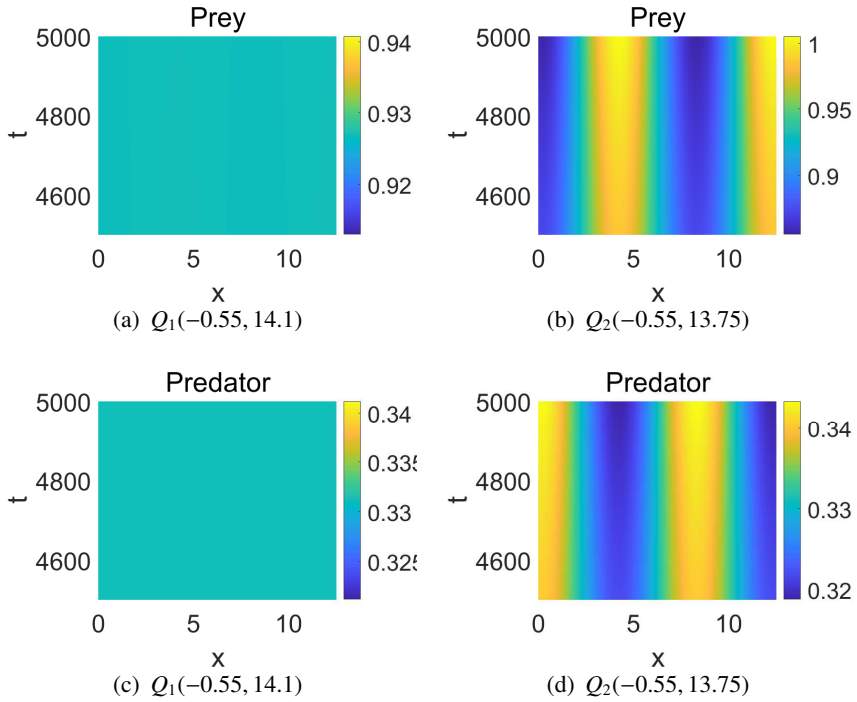


(a) $Q_1(-0.55, 14.1)$ (b) $Q_2(-0.55, 13.75)$

(c) $Q_1(-0.55, 14.1)$ (d) $Q_2(-0.55, 13.75)$

**Figure 2.** Numerical simulations of system (1.2) with $\sigma = 0$ for $(d_{21}, \tau)$ chosen as $Q_i (i = 1, 2)$ in Figure 1, showing spatially homogeneous and nonhomogeneous steady states. The initial conditions are chosen as (a)–(b): $u(x, 0) = 0.9268 + 0.01\cos(3x/4)$; (c)–(d): $v(x, 0) = 0.3312 + 0.01\cos(3x/4)$.

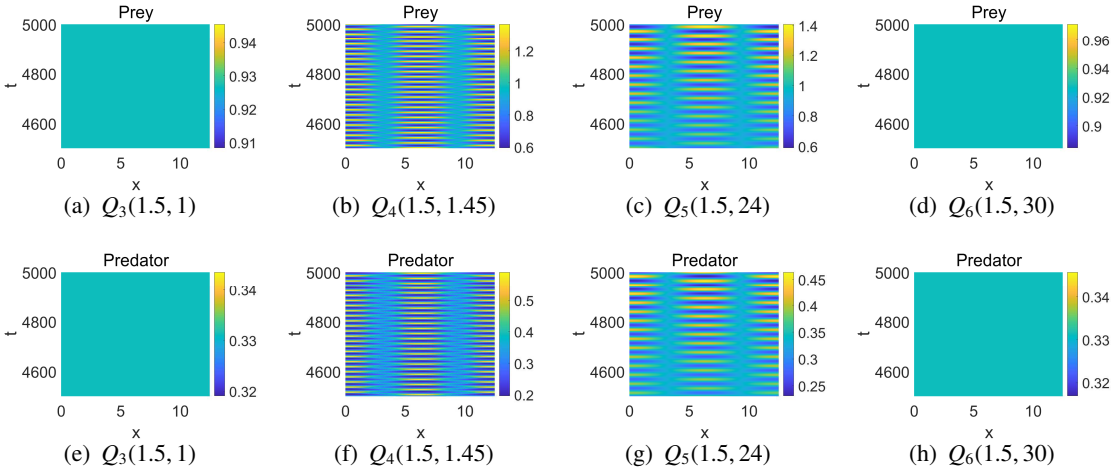


(a) $Q_3(1.5, 1)$ (b) $Q_4(1.5, 1.45)$ (c) $Q_5(1.5, 24)$ (d) $Q_6(1.5, 30)$

(e) $Q_3(1.5, 1)$ (f) $Q_4(1.5, 1.45)$ (g) $Q_5(1.5, 24)$ (h) $Q_6(1.5, 30)$

**Figure 3.** Numerical simulations of system (1.2) with $\sigma = 0$ for $(d_{21}, \tau)$ chosen as $Q_i (i = 3, 4, 5, 6)$ in Figure 1, showing spatially homogeneous steady states and nonhomogeneous periodic patterns. The initial conditions are chosen as (a)–(d): $u(x, 0) = 0.9268 + 0.01\cos(3x/4)$; (e)–(h): $v(x, 0) = 0.3312 + 0.01\cos(3x/4)$.

which implies that the spatially nonhomogeneous Hopf bifurcation at $\tau = \tau_*$ is supercritical and stable.

For $\tau_H = \tau^* \approx 27.1474$,

$$\kappa_1 \approx -0.0027 < 0, \kappa_2 \approx -0.0066 < 0,$$

which implies that the spatially nonhomogeneous Hopf bifurcation at $\tau = \tau^*$ is subcritical and stable. When $\tau = 1 < \tau_*$, $E_*$ is spatially homogeneous steady state (see Figure 3(a),(e)). Letting $\tau_* < \tau = 1.45 < \tau^*$ (but close to $\tau_*$), $E_*$ is the mode-2 spatially nonhomogeneous periodic solution (see Figure 3(b),(f)), the point $(d_{21}, \tau) \approx (1, 5, 1.45)$ may correspond to a subcritical Hopf bifurcation. For $\tau_* < \tau = 24 < \tau^*$ (but close to $\tau^*$), $E_*$ is the mode-2 spatially Hopf bifurcation (see Figure 3(c),(g)). When $\tau = 30 > \tau^*$, $E_*$ is spatially homogeneous steady state (see Figure 3(d),(h)).

Through numerical simulation, the green and blue areas are the stability region of the positive equilibrium $E_*$ in Figure 1. When points $Q_1$, $Q_3$, and $Q_6$ are selected in the stability region, the positive equilibrium is locally asymptotically stable, as shown in Figure 2(a),(c), Figure 3(a),(e), and Figure 3(d),(h). When $(d_{21}, \tau)$ crosses the boundary of the stability region, points $Q_2$, $Q_4$, and $Q_5$ are selected. The system (1.2) exhibits Turing bifurcation and Hopf bifurcation at the positive equilibrium $E_*$, as illustrated in Figure 2(b),(d), Figure 3(b),(f), and Figure 3(c),(g).

### *4.2. The Spatiotemporal distribution when $\sigma > 0$*

In terms of Theorems 2.5 and 2.9, for $(d_{21}, \tau) \in E_s \cup E_c \cup E_h$ and $\sigma = 0$, $E_*$ is stable. Now, we study whether $E_*$ becomes unstable again when the gestation delay $\sigma \geq 0$. In what follows, we always fix $d_{21}$, dividing it into three cases:

$$(\mathrm{I}) d_{21} < d_S^*; (\mathrm{II}) d_S^* < d_{21} < d_H^*; (\mathrm{III}) d_{21} > d_H^*.$$

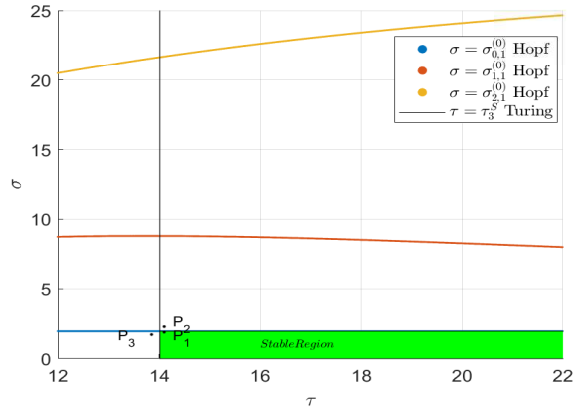


**Figure 4.** Bifurcation diagram in the plane of $\tau - \sigma$ for fixed $d_{21} = -0.55$, in which the Hopf bifurcation curves are $\sigma = \sigma_{n,1}^{(0)}, n = 0, 1, 2$, and the Turing bifurcation curve is $\tau = \tau_3^S$. The Hopf bifurcation curve $\sigma = \sigma_{0,1}^{(0)}$ and the Turing bifurcation curve $\tau = \tau_3^S$ intersect at the point $P_*(14.0143, 1.9719)$. The points $P_1(14.1, 1.9)$, $P_2(14.1, 2.3)$, $P_3(13.85, 1.73)$ are chosen for the numerical simulations.

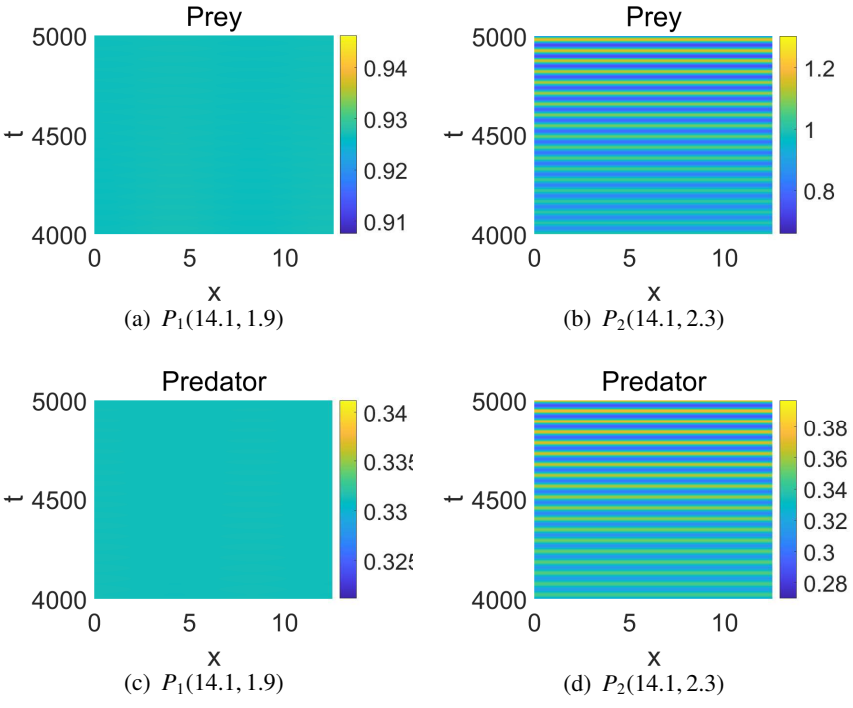


(a) $P_1(14.1, 1.9)$ (b) $P_2(14.1, 2.3)$

(c) $P_1(14.1, 1.9)$ (d) $P_2(14.1, 2.3)$

**Figure 5.** Numerical simulations of system (1.2) for $(d_{21}, \tau)$ chosen as $P_i (i = 1, 2)$ in Figure 2, showing spatially homogeneous steady state and homogeneous periodic pattern. The initial conditions are chosen as (a)–(b): $u(x, 0) = 0.9268 + 0.01\cos(3x/4)$; (c)—(d): $v(x, 0) = 0.3312 + 0.01\cos(3x/4)$.

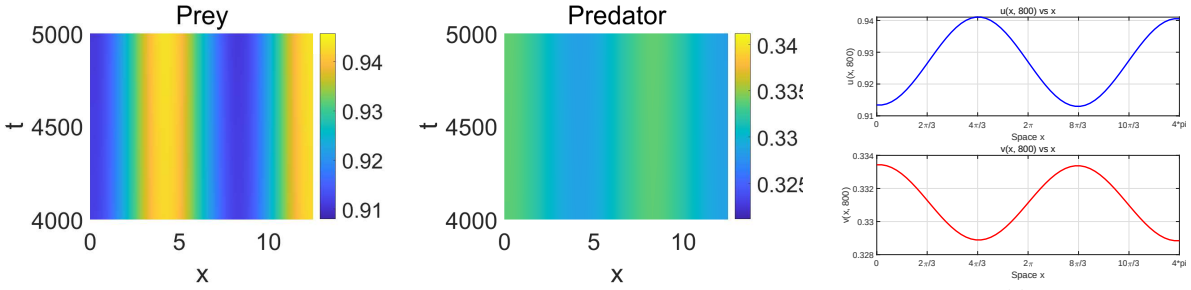


(a) $P_3(13.85, 1.73)$ (b) $P_3(13.85, 1.73)$ (c)

**Figure 6.** Numerical simulations of system (1.2) with $\sigma > 0$ for $(d_{21}, \tau)$ chosen as $P_3$ in Figure 4, showing spatially homogeneous Hopf bifurcation. The initial conditions are chosen as (a): $u(x, 0) = 0.9268 + 0.01\cos(3x/4)$; (b): $v(x, 0) = 0.3312 + 0.01\cos(3x/4)$. (c): The truncated curves of (a) and (b) for fixed $t = 800$.

#### 4.2.1. $d_{21} = -0.55 < d_S^*$

According to Theorem 2.5, for $\sigma = 0$, when $d_{21} < d_S^* \approx -0.1791$, $E_*$ is locally asymptotically stable for $\tau > \tau_S$ and unstable for $0 < \tau < \tau_S$. From Theorem 2.15, for $d_{21} = -0.55 < d_S^*$, $E_*$ always is unstable when $0 < \tau < \tau_S$ and $\sigma \geq 0$. Thus, we concentrate on observing the cases of $\tau > \tau_S$ and $\sigma \geq 0$. In terms of mathematical analysis, for $\tau > \tau_S = 14.0143$, we will show the occurrence of Hopf bifurcation for $\sigma$ as larger than some value $\sigma_*$; meanwhile, for $\tau = \tau_S = 14.0143$, we shall declare the occurrence of Turing–Hopf bifurcation for some value of $\sigma_*$.

From Lemma 2.12, for fixed $\tau \in (12, 22)$ and $d_{21} = -0.55$, Eq (2.38) with coefficient (2.39) has no positive real roots when $\sigma \geq 0$ and $n > N_* = 3$, and we plot a series of Hopf bifurcation curves $\sigma = \sigma_{n,1}^{(0)}(n = 0, 1, 2)$ and the Turing bifurcation curve $\tau = \tau_S \approx 14.0143$ in Figure 4. Therefore, $P_*(14.0143, 1.9719)$ is the intersection of curve $\sigma = \sigma_{0,1}^{(0)}$ and $\tau \approx 14.0143$, that is called Turing–Hopf bifurcation point. Together with (2.46), we obtain $\sigma_* = 1.9719$. Near $P_*$, $P_i(i = 1, 2, 3)$ are chosen for the numerical simulations. For fixed $\tau = 14.1 > \tau_S$, $E_*$ is homogeneous steady state when $\sigma = 1.9 < \sigma_*$ (see Figure 5(a),(c)); $E_*$ is spatially homogeneous periodic solution when $\sigma = 2.3 > \sigma_*$ (see Figure 5(b),(d)). For fixed $\tau = 13.85 < \tau_S$, $E_*$ is spatially homogeneous Hopf bifurcation (see Figure 6(a),(b)).

#### 4.2.2. $d_S^* < d_{21} = 0.75 < d_H^*$

Let memory diffusion coefficient $d_S^* \approx -0.1791 < d_{21} = 0.75 < d_H^* \approx 0.8006$, then from Theorems 2.5 and 2.9, $E_*$ is stable for any $\tau \geq 0$ and $\sigma = 0$. Similarly, fixed $\tau \in (0, 40)$ and $d_{21} = 0.75$, when $\sigma \geq 0$ and $n > N_* = 3$, Eq (2.38) with coefficient (2.39) has no positive real roots. Then, following from (2.44), we plot a series of Hopf bifurcation curves $\sigma = \sigma_{n,1}^{(0)}(n = 0, 1, 2)$ (see Figure 7).

When $\tau = 12$, we calculate that from (2.41) that

$$v_{1,1}^2 = z_{1,1} \approx 0.0194, L'(z_{1,1}) \approx 0.0009 > 0,$$

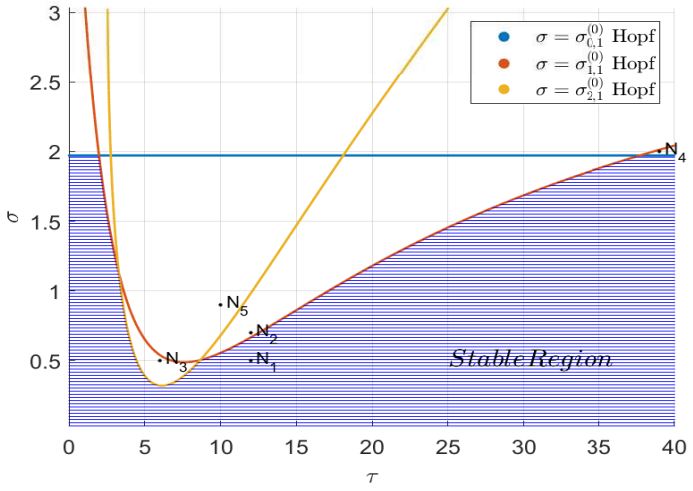


**Figure 7.** Bifurcation diagram in the plane of $\tau - \sigma$ for fixed $d_{21} = 0.75$, in which the Hopf bifurcation curves are $\sigma = \sigma^{(0)}_{n,1}, n = 0, 1, 2$. The points $N_1(12, 0.5)$, $N_2(12, 0.7)$, $N_3(6, 0.5)$, $N_4(39, 2)$, $N_5(10, 0.9)$ are chosen for the numerical simulations.

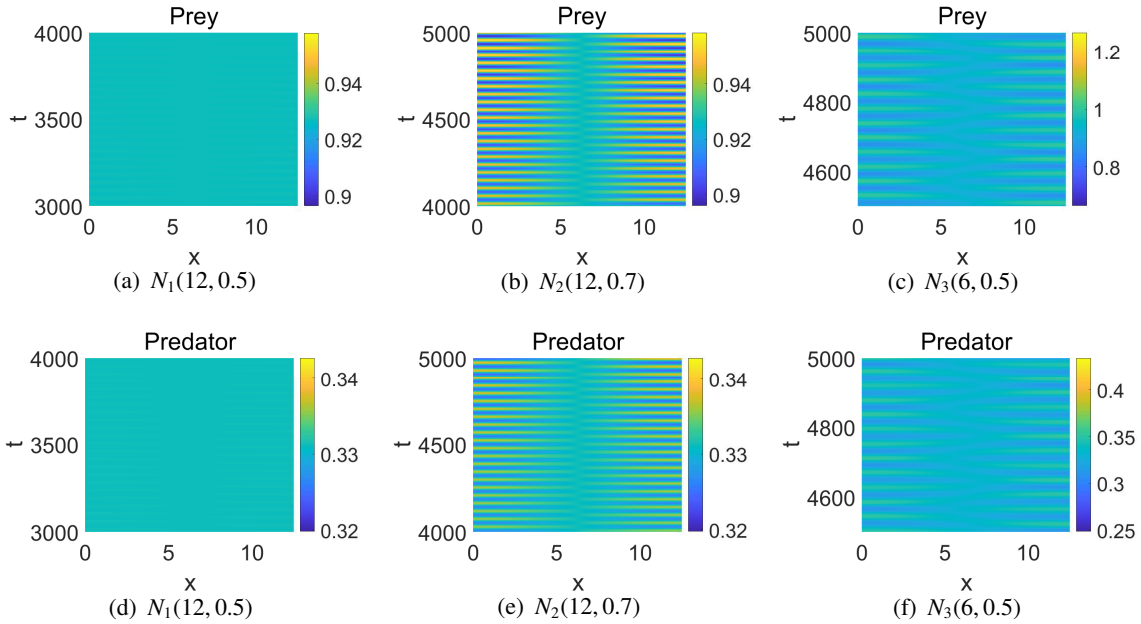


(a) $N_1(12, 0.5)$ (b) $N_2(12, 0.7)$ (c) $N_3(6, 0.5)$

(d) $N_1(12, 0.5)$ (e) $N_2(12, 0.7)$ (f) $N_3(6, 0.5)$

**Figure 8.** Numerical simulations of system (1.2) for $(\tau, \sigma)$ chosen as $N_i (i = 1, 2, 3)$ in Figure 7, showing spatially homogeneous steady state and nonhomogeneous periodic patterns. The initial conditions are chosen as (a)–(b): $u(x, 0) = 0.9268 + 0.01\cos(3x/4)$, (c): $u(x, 0) = 0.9268 + 0.01\cos(x/4)$; (d)–(e): $v(x, 0) = 0.3312 + 0.01\cos(3x/4)$, (f): $v(x, 0) = 0.3312 + 0.01\cos(x/4)$.

which implies from Lemma 2.14 that

$$\operatorname{sign}\left(\left.\frac{\mathrm{d}\,\mathrm{Re}(\lambda(\sigma))}{\mathrm{d}\sigma}\right|_{\sigma=\sigma_{1,1}^{(0)}}\right)=\operatorname{sign}\left(L'\left(z_{1,1}\right)\right)>0.$$

In addition, it follows by (2.46) that

$$\sigma_*=\min_{0\le n\le 2,k=1,2,3}\sigma_{n,k}^{(0)}=\sigma_{1,1}^{(0)}\approx 0.666850,$$

hence for $\sigma=0.5<\sigma_*$, $E_*$ is spatially homogeneous steady state (see Figure 8(a),(d)); for $\sigma=0.7>\sigma_*$, $E_*$ is the mode-1 spatially nonhomogeneous periodic solution (see Figure 8(b),(e)).

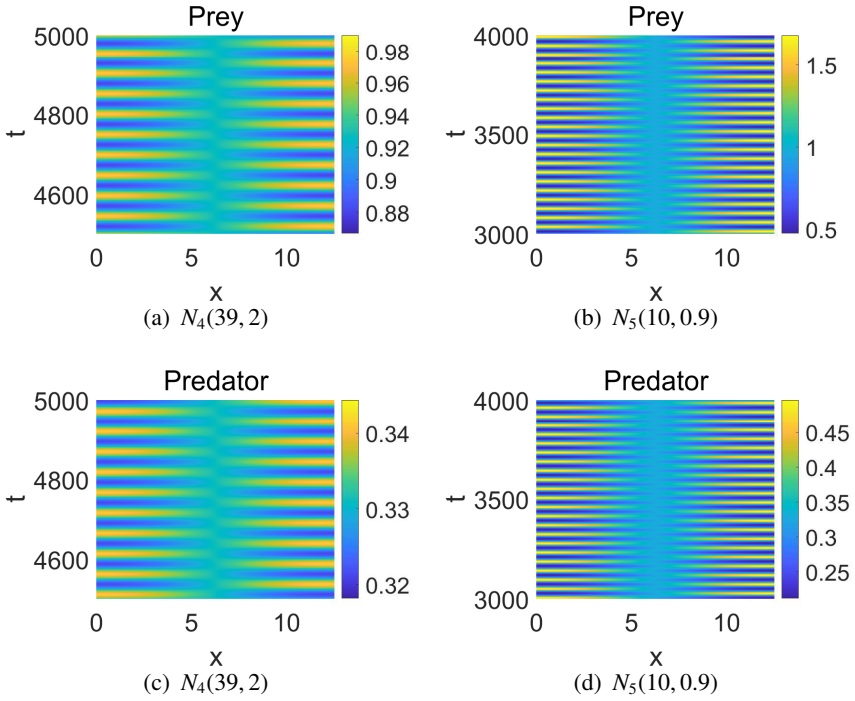


(a) $N_4(39,2)$ (b) $N_5(10,0.9)$

(c) $N_4(39,2)$ (d) $N_5(10,0.9)$

**Figure 9.** Numerical simulations of system (1.2) for $(\tau,\sigma)$ chosen as $N_i(i=4,5)$ in Figure 7, showing nonhomogeneous periodic patterns. The initial conditions are chosen as (a): $u(x,0)=0.9268+0.01\cos(x/4)$, (b): $u(x,0)=0.9268+0.01\cos(3x/4)$; (c): $v(x,0)=0.3312+0.01\cos(x/4)$, (d): $v(x,0)=0.3312+0.01\cos(3x/4)$.

When $\tau=6$, we can get from (2.46) that

$$\sigma_*=\min_{0\le n\le 2,k=1,2,3}\sigma_{n,k}^{(0)}=\sigma_{2,1}^{(0)}\approx 0.320966,$$

and

$$\operatorname{sign}\left(\left.\frac{\mathrm{d}\,\mathrm{Re}(\lambda(\sigma))}{\mathrm{d}\sigma}\right|_{\sigma=\sigma_{2,1}^{(0)}}\right)=\operatorname{sign}\left(L'\left(z_{2,1}\right)\right)=0.0029>0,$$

hence for $\sigma=0.5>\sigma_*$, $E_*$ is the mode-2 spatially nonhomogeneous periodic solution (see Figure 8(c),(f)).

When $\tau = 39$, similarly, we calculate from (2.46) that

$$\sigma_* = \min_{0\le n\le 2, k=1,2,3} \sigma_{n,k}^{(0)} = \sigma_{0,1}^{(0)} \approx 1.971880,$$

hence for $\sigma = 2 > \sigma_*$, $E_*$ is spatially nonhomogeneous periodic solution (see Figure 9(a),(c)). Similarly, $E_*$ is spatially nonhomogeneous periodic solution (see Figure 9(b),(d)).

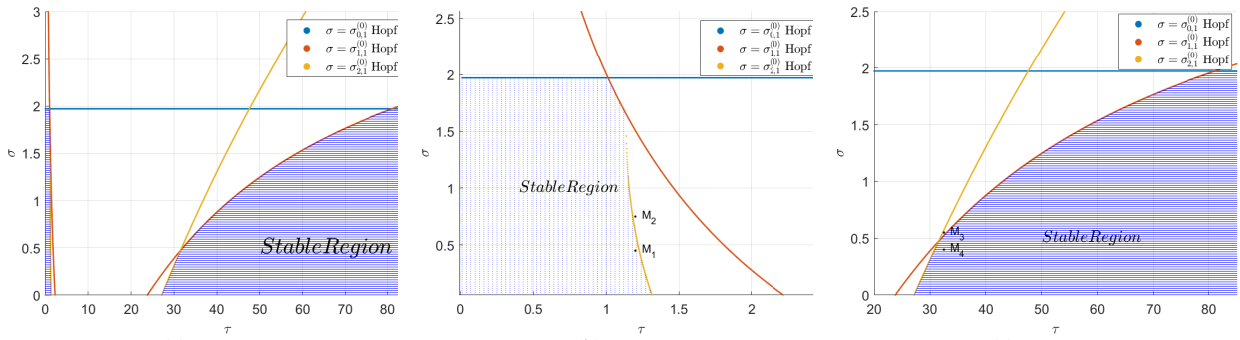


(a) (b) (c)

**Figure 10.** Bifurcation diagram in the plane of $\tau - \sigma$ for fixed $d_{21} = 1.5$ in which the Hopf bifurcation curves are $\sigma = \sigma_{n,1}^{(0)}, n = 0, 1, 2$. The points $M_1(1.2, 0.45)$, $M_2(1.2, 0.75)$, $M_3(32.5, 0.55)$, and $M_4(32.5, 0.4)$ are chosen for the numerical simulations. Figure 10(b) and (c) are the enlargement of Figure 10(a) restricted to the region $0 < d_{21} < 2.5, 0 < \tau < 2.5$ and $20 < d_{21} < 85, 0 < \tau < 2.5$, respectively.

4.2.3. $d_{21} = 1.5 > d_H^*$

According to Theorem 2.9, when $d_{21} = 1.5 > d_H^* \approx 0.8006$ for $\sigma = 0$, $E_*$ is stable for any $0 \le \tau < \tau_* \approx 1.3313$ and $\tau > \tau^* \approx 27.1474$, and unstable $\tau \in (\tau_*, \tau^*) \approx (1.3313, 27.1474)$. Fixed $\tau \in (0, 85)$ and $d_{21} = 1.5$, when $\sigma \ge 0$ and $n > N_* = 3$, Eq (2.38) with coefficient (2.39) has no positive real roots. Then from (2.44), we plot a series of Hopf bifurcation curves $\sigma = \sigma_{n,1}^{(0)} (n = 0, 1, 2)$ (see Figure 10).

For fixed $\tau = 1.2 < \tau_*$, we calculate from (2.46) that

$$\sigma_* = \min_{0\le n\le 2, k=1,2,3} \sigma_{n,k}^{(0)} = \sigma_{2,1}^{(0)} \approx 0.614854,$$

hence for $\sigma = 0.45 < \sigma_*$, $E_*$ is spatially homogeneous steady state (see Figure 11(a),(e)); for $\sigma = 0.75 > \sigma_*$, $E_*$ is the mode-2 spatially nonhomogeneous periodic solution (see Figure 11(b),(f)).

For fixed $\tau = 32.5 > \tau^*$, we calculate from (2.46) that

$$\sigma_* = \min_{0\le n\le 2, k=1,2,3} \sigma_{n,k}^{(0)} = \sigma_{1,1}^{(0)} \approx 0.524696,$$

so for $\sigma = 0.55 > \sigma_*$, $E_*$ is the mode-1 spatially nonhomogeneous periodic solution (see Figure 11(c),(g)); $E_*$ is spatially homogeneous steady state when $\sigma = 0.4 < \sigma_*$ (see Figure 11(d),(h)).

Through numerical simulation, we take $d_{21}$ as the bifurcation parameter and analyze the following three cases: $d_{21} = -0.55 < d_S^*$, $d_S^* < d_{21} = 0.75 < d_H^*$, and $d_{21} = 1.5 > d_H^*$ (see Figures 4, 7 and 10). In

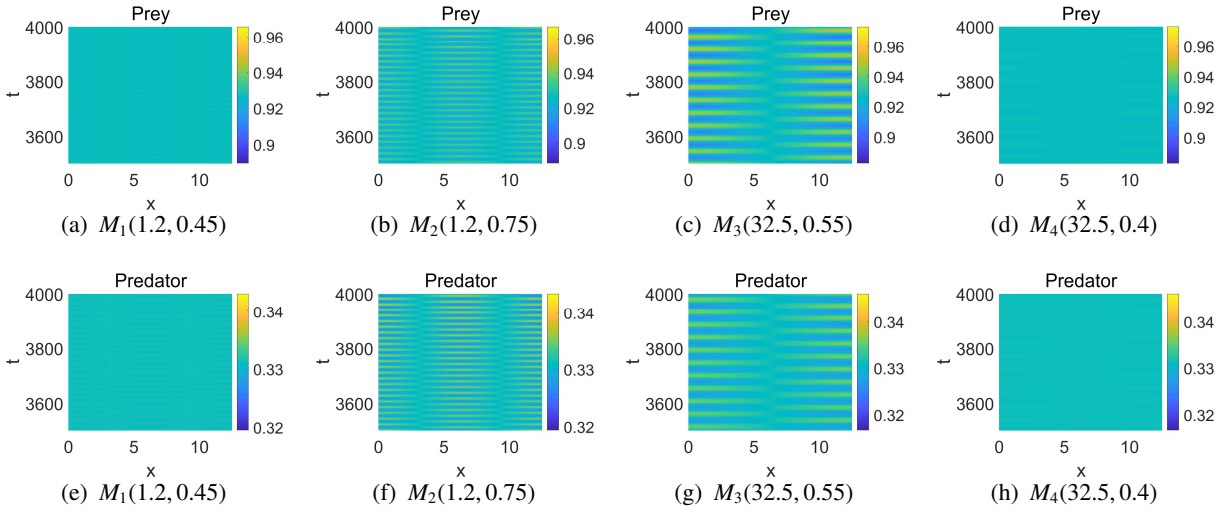


(a) $M_1(1.2, 0.45)$ (b) $M_2(1.2, 0.75)$ (c) $M_3(32.5, 0.55)$ (d) $M_4(32.5, 0.4)$

(e) $M_1(1.2, 0.45)$ (f) $M_2(1.2, 0.75)$ (g) $M_3(32.5, 0.55)$ (h) $M_4(32.5, 0.4)$

**Figure 11.** Numerical simulations of system (1.2) with $\sigma > 0$ for $(\tau, \sigma)$ chosen as $M_i (i = 1, 2, 3, 4)$ in Figure 10, showing spatially homogeneous steady states and nonhomogeneous periodic patterns. The initial conditions are chosen as (a)–(b): $u(x, 0) = 0.9268 + 0.01\cos(x/4)$; (c)–(d): $u(x, 0) = 0.9268 + 0.01\cos(3x/4)$; (e)–(f): $v(x, 0) = 0.3312 + 0.01\cos(x/4)$; (g)–(h): $v(x, 0) = 0.3312 + 0.01\cos(3x/4)$.

each case, there exist stable regions. Within the stable regions of each case, the positive equilibrium $E_*$ is locally asymptotically stable, as illustrated in Figure 5(a),(c), Figure 8(a),(d), and Figure 11(a),(e). In contrast, when $(\tau, \sigma)$ crosses the boundary of the stable region, the stability of $E_*$ changes, and the positive equilibrium $E_*$ manifests as either spatially homogeneous or nonhomogeneous periodic solutions.

## 5. Conclusions

In this paper, we propose a diffusive predator-prey model with the distributed delay $\tau$ and the gestation delay $\sigma$. Firstly, we present the conditions for the occurrence of Hopf bifurcation and Turing bifurcation at the positive equilibrium $E_*$ of system (1.2). When $\sigma = 0$, for $d_{21} < d_S^*$, the positive equilibrium $E_*$ of system (1.2) undergoes Turing bifurcation at $\tau = \tau_S$; for $d_{21} > d_H^*$, the positive equilibrium of system (1.2) undergoes Hopf bifurcation at $\tau = \tau_*(\tau = \tau^*)$. When $\sigma > 0$, for $d_S^* < d_{21} < d_H^*$, there exists a critical value $\sigma_*$ of $\sigma$ such that the positive equilibrium $E_*$ of system (1.2) undergoes Hopf bifurcation at $\sigma = \sigma_*$; for $d_{21} < d_S^*$, the positive equilibrium $E_*$ of system (1.2) undergoes Turing–Hopf bifurcation at $(\tau, \sigma) = (\tau_S, \sigma_{n,k}^{(j)})$, where $n \in \mathbb{N}_0$, $j \in \mathbb{N}$, and $k = 1, 2, 3$; for $d_{21} > d_H^*$, there also exists a critical value $\sigma_*$ of $\sigma$ such that the positive equilibrium $E_*$ of system (1.2) undergoes Hopf bifurcation at $\sigma = \sigma_*$. Secondly, when $\sigma = 0$, we calculate the normal form of Hopf bifurcation induced by the memory delay, and study the direction and stability of Hopf bifurcation. Finally, the numerical simulation results validate theoretical findings. Variations in the memory-based diffusion coefficient, memory delay, and gestation delay may induce transitions between spatially homogeneous or nonhomogeneous steady states and spatially homogeneous or nonhomogeneous periodic solutions.

In order to maintain ecological balance and protect biological diversity, we hope that prey and predator can coexist and their numbers remain relatively stable. The density of prey and predator populations approaches a relatively stable state when $(\tau, \sigma)$ is in the stable region, while it fluctuates when $(\tau, \sigma)$ is outside the stable region. Therefore, by adjusting the gestation delay of predator and the memory of predator on distribution of prey, the population densities can be made to tend towards a stable state. Besides, the size of the stable region is affected by other parameters of the system, such as the memory-based diffusion coefficient $d_{21}$. According to memory, the prey moves to a relatively safe area with fewer predators in order to avoid predation. Predators also remember the historical distribution of the prey in space to improve their capture rate. Thus, we can take appropriate measures to control the memory diffusion coefficient of species to expand the stable region of the positive equilibrium.

In this paper, we calculated the normal form of Hopf bifurcation induced by the distributed memory delay $\tau$ when the gestation delay $\sigma = 0$. In future work, we hope to calculate the normal forms of Turing and Turing–Hopf bifurcations when the memory delay $\tau \neq 0$ and the gestation delay $\sigma \neq 0$. Moreover, the kernel function used in this paper is a weak kernel function. Exploring the impact of strong or other kernel functions on the spatial patterns of the system is an worthwhile topic for future research.

## Use of AI tools declaration

The authors declare they have not used Artificial Intelligence (AI) tools in the creation of this article.

## Acknowledgments

This work was supported by the National Natural Science Foundation of China (No.11761040). We greatly appreciate the editors' and the anonymous referees' careful reading and helpful suggestions which have made the manuscript a real significant improvement.

## Conflict of interest

The authors declare there are no conflicts of interest.

## References

1. Q. Zhu, F. Chen, Impact of fear on searching efficiency of first species: A two species Lotka-Volterra competition model with weak Allee effect, *Qual. Theory Dyn. Syst.*, **23** (2024), 143. https://doi.org/10.1007/s12346-024-01000-4
2. H. Zhang, H. Qi, Hopf bifurcation analysis of a predator-prey model with prey refuge and fear effect under non-diffusion and diffusion, *Qual. Theory Dyn. Syst.*, **22** (2023), 135. https://doi.org/10.1007/s12346-023-00837-5
3. S. K. Sasmal, Population dynamics with multiple Allee effects induced by fear factors-A mathematical study on prey-predator interactions, *Appl. Math. Model.*, **64** (2018), 1–14. https://doi.org/10.1016/j.apm.2018.07.021

4. Y. Li, M. He, Z. Li, Dynamics of a ratio-dependent Leslie-Gower predator-prey model with Allee effect and fear effect, *Math. Comput. Simul.*, **201** (2022), 417–439. https://doi.org/10.1016/j.matcom.2022.05.017
5. H. Mo, Y. Shao, Stability and bifurcation analysis of a delayed stage-structured predator-prey model with fear, additional food, and cooperative behavior in both species, *Adv. Cont. Discr. Mod.*, **2025** (2025), 27. https://doi.org/10.1186/s13662-025-03879-y
6. W. Kong, Y. Shao, Bifurcations of a Leslie-Gower predator-prey model with fear, strong Allee effect and hunting cooperation, *AIMS Math.*, **7** (2024), 31607–31635. https://doi.org/10.3934/math.20241520
7. W. Li, L. Zhang, J. Cao, A note on Turing-Hopf bifurcation in a diffusive Leslie-Gower model with weak Allee effect on prey and fear effect on predator, *Appl. Math. Lett.*, **172** (2026), 109741. https://doi.org/10.1016/j.aml.2025.109741
8. P. A. Stephens, W. J. Sutherland, Consequences of the Allee effect for behaviour, ecology and conservation, *Trends Ecol. Evol.*, **14** (1999), 401–405. https://doi.org/10.1016/S0169-5347(99)01684-5
9. F. Courchamp, T. Clutton-Brock, B. Grenfell, Inverse density dependence and the Allee effect, *Trends Ecol. Evol.*, **14** (1999), 405–410. https://doi.org/10.1016/S0169-5347(99)01683-3
10. W. C. Allee, Animal aggregations, *Q. Rev. Biol.*, **2** (1927), 367–398. https://doi.org/10.1086/394281
11. P. Shri Harine, A. Kumar, K. P. Reshma, Local and global dynamics of a prey-predator system with fear, Allee effect, and variable attack rate, *Chaos Interdiscip. J. Nonlinear Sci.*, **34** (2024), 93126. https://doi.org/10.1063/5.0227458
12. Q. An, C. Wang, H. Wang, Analysis of a spatial memory model with nonlocal maturation delay and hostile boundary condition, *Discrete Contin. Dyn. Syst. A*, **40** (2020), 5845–5868. https://doi.org/10.3934/dcds.2020249
13. S. Li, Z. Li, B. Dai, Stability and Hopf bifurcation in a prey-predator model with memory-based diffusion, *Discrete Contin. Dyn. Syst. B*, **27** (2022), 6885-6906. https://doi.org/10.3934/dcdsb.2022025
14. M. Liu, H. Wang, W. Jiang, Bifurcations and pattern formation in a predator-prey model with memory-based diffusion, *J. Differ. Equations*, **350** (2023), 1–40. https://doi.org/10.1016/j.jde.2022.12.010
15. W. Zhang, D. Jin, R. Yang, Hopf bifurcation in a predator-prey model with memory effect in predator and anti-predator behaviour in prey, *Mathematics*, **11** (2023), 556. https://doi.org/10.3390/math11030556
16. X. Zhang, H. Zhu, Q. An, Dynamics analysis of a diffusive predator-prey model with spatial memory and nonlocal fear effect, *J. Math. Anal. Appl.*, **525** (2023), 127123. https://doi.org/10.1016/j.jmaa.2023.127123
17. M. Wu, H. Yao, Bifurcation analysis of a delayed diffusive predator-prey model with spatial memory and toxins, *Z. Angew. Math. Phys.*, **75** (2024), 25. https://doi.org/10.1007/s00033-023-02157-9

18. W. F. Fagan, M. A. Lewis, M. Auger-Méthé, T. Avgar, S. Benhamou, G. Breed, et al., Spatial memory and animal movement, *Ecol. Lett.*, **16** (2013), 1316–1329. https://doi.org/10.1111/ele.12165
19. J. Shi, C. Wang, H. Wang, X. Yan, Diffusive spatial movement with memory, *J. Dyn. Differ. Equations*, **32** (2020), 979–1002. https://doi.org/10.1007/s10884-019-09757-y
20. Y. Song, J. Shi, H. Wang, Spatiotemporal dynamics of a diffusive consumer-resource model with explicit spatial memory, *Stud. Appl. Math.*, **148** (2022), 373–395. https://doi.org/10.1111/sapm.12443
21. H. Shen, Y. Song, H. Wang, Bifurcations in a diffusive resource-consumer model with distributed memory, *J. Differ. Equations*, **347** (2023), 170–211. https://doi.org/10.1016/j.jde.2022.11.044
22. U. E. Schlägel, M. A. Lewis, Detecting effects of spatial memory and dynamic information on animal movement decisions, *Methods Ecol. Evol.*, **5** (2014), 1236–1246. https://doi.org/10.1111/2041-210X.12284
23. S. Li, S. Yuan, Z. Jin, H. Wang, Bifurcation analysis in a diffusive predator-prey model with spatial memory of prey, Allee effect and maturation delay of predator, *J. Differ. Equations*, **357** (2023), 32–63. https://doi.org/10.1016/j.jde.2023.02.009
24. C. Wang, S. Yuan, H. Wang, Spatiotemporal patterns of a diffusive prey-predator model with spatial memory and pregnancy period in an intimidatory environment, *J. Math. Biol.*, **84** (2022), 12. https://doi.org/10.1007/s00285-022-01716-4
25. H. Shen, Y. Song, Spatiotemporal patterns in a diffusive resource-consumer model with distributed memory and maturation delay, *Math. Comput. Simul.*, **221** (2024), 622–644. https://doi.org/10.1016/j.matcom.2024.03.026
26. T. Faria, Normal forms and Hopf bifurcation for partial differential equations with delays, *Trans. Am. Math. Soc.*, **352** (2000), 2217–2238. https://doi.org/10.1090/S0002-9947-00-02280-7
27. S. Wu, Y. Song, Spatiotemporal dynamics of a diffusive predator-prey model with nonlocal effect and delay, *Commun. Nonlinear Sci. Numer. Simul.*, **89** (2020), 105310. https://doi.org/10.1016/j.cnsns.2020.105310
28. S. Ruan, On the zeros of a third degree exponential polynomial with applications to a delayed model for the control of testosterone secretion, *Math. Med. Biol.*, **18** (2001), 41–52. https://doi.org/10.1093/imammb/18.1.41
29. Q. Shi, J. Shi, H. Wang, Spatial movement with distributed memory, *J. Math. Biol.*, **82** (2021), 33. https://doi.org/10.1007/s00285-021-01588-0
30. T. Faria, L. T. Magalhaes, Normal forms for retarded functional differential equations with parameters and applications to Hopf bifurcation, *J. Differ. Equ.*, **122** (1995), 181–200. https://doi.org/10.1006/jdeq.1995.1144
31. Y. Song, Y. Peng, T. Zhang, The spatially inhomogeneous Hopf bifurcation induced by memory delay in a memory-based diffusion system, *J. Differ. Equations*, **300** (2021), 597–624. https://doi.org/10.1016/j.jde.2021.08.010
32. S. Wiggins, *Introduction to Applied Nonlinear Dynamical Systems and Chaos*, Springer-Verlag, New York, 2003. https://doi.org/10.1007/b97481

## Appendix

We can deduce from (3.3) that

$$F_2(\psi) = f_{200}\psi_1^2 + f_{020}\psi_1^2 + 2f_{110}\psi_1\psi_2, \tag{A.1}$$

and

$$F_3(\psi) = f_{300}\psi_1^3 + f_{030}\psi_2^3 + 3f_{120}\psi_1\psi_2^2 + 3f_{210}\psi_1^2\psi_2. \tag{A.2}$$

Here,

$$f_{110} = \begin{pmatrix} -\frac{rk}{(1+kv_*)^2} - \frac{au_*(u_*+2c)}{(bu_*^2+u_*+c)^2} \\ \frac{\eta a u_* v_*(u_*+2c)}{(\theta+v_*)(bu_*^2+u_*+c)^2} + \frac{\eta\theta a u_* v_*(u_*+2c)}{(\theta+v_*)^2(bu_*^2+u_*+c)^2} \\ 0 \end{pmatrix}, f_{020} = \begin{pmatrix} \frac{rk^2u_*}{(1+kv_*)^3} \\ -\frac{\theta\eta a u_*^2 v_*}{(1+kv_*)^3(bu_*^2+u_*+c)} + \frac{\eta\theta a u_*^2}{(\theta+v_*)^2(bu_*^2+u_*+c)} \\ 0 \end{pmatrix},$$

$$f_{030} = \begin{pmatrix} -\frac{r_1 u_* k^3}{(1+kv_*)^4} \\ \frac{\theta\eta a u_*^2 v_*}{(\theta+v_*)^4(bu_*^2+u_*+c)} - \frac{\theta\eta a u_*^2}{(\theta+v_*)^3(bu_*^2+u_*+c)} \\ 0 \end{pmatrix}, f_{120} = \begin{pmatrix} \frac{rk^2}{(1+kv_*)^3} \\ \frac{\eta a u_*\theta(u_*+2c)}{(\theta+v_*)^2(bu_*^2+u_*+c)^2} - \frac{\eta\theta a u_* v_*(u_*+2c)}{(\theta+v_*)^3(bu_*^2+u_*+c)^2} \\ 0 \end{pmatrix},$$

$$f_{210} = \begin{pmatrix} \frac{a(bu_*^3+3bcu_*^2-c^2)}{(bu_*^2+u_*+c)^3} \\ -\frac{\theta\eta a v_*(bu_*^3+3bcu_*^2-c^2)}{(\theta+v_*)^2(bu_*^2+u_*+c)^3} - \frac{\eta a v_*(bu_*^3+3bcu_*^2-c^2)}{(\theta+v_*)(bu_*^2+u_*+c)^3} \\ 0 \end{pmatrix}, f_{200} = \begin{pmatrix} -r_1 + \frac{a v_*(bu_*^3+3bcu_*^2-c^2)}{(bu_*^2+u_*+c)^3} \\ -\frac{\eta a v_*^2(bu_*^3+3bcu_*^2-c^2)}{(\theta+v_*)(bu_*^2+u_*+c)^3} \\ 0 \end{pmatrix},$$

$$f_{300} = \begin{pmatrix} -\frac{a v_*(b^2u_*^4+4u_*^3b^2c-4u_*bc^2-c^2)}{(bu_*^2+u_*+c)^4} \\ \frac{\eta a v_*^2(b^2u_*^4+4u_*^3b^2c-4u_*bc^2-c^2)}{(\theta+v_*)(bu_*^2+u_*+c)^4} \\ 0 \end{pmatrix}.$$

Letting

$$\psi = \mathcal{P}\omega b_{n_H}(x) = \begin{pmatrix} p_1\omega_1 b_{n_H}(x) + \bar{p}_1\omega_2 b_{n_H}(x) \\ p_2\omega_1 b_{n_H}(x) + \bar{p}_2\omega_2 b_{n_H}(x) \\ p_3\omega_1 b_{n_H}(x) + \bar{p}_3\omega_2 b_{n_H}(x) \end{pmatrix} = \begin{pmatrix} \psi_1 \\ \psi_2 \\ \psi_3 \end{pmatrix}, \tag{A.3}$$

we have

$$F_2(\mathcal{P}\omega b_{n_H}(x)) = \sum_{r_1+r_2=2} \mathcal{A}_{r_1r_2}\omega_1^{r_1}\omega_2^{r_2} b_{n_H}^2(x), \tag{A.4}$$

then in conjunction with (A.1), (A.3), and (A.4), we obtain

$$\begin{aligned} &\mathcal{A}_{20} = f_{200}p_1^2 + 2f_{110}p_1p_2 + f_{020}p_2^2, \mathcal{A}_{02} = f_{200}\bar{p}_1^2 + f_{020}\bar{p}_2^2 + 2f_{110}\bar{p}_1\bar{p}_2, \\ &\mathcal{A}_{11} = 2f_{200}p_1\bar{p}_1 + 2f_{020}p_2\bar{p}_2 + 2f_{110}(\bar{p}_1p_2 + p_1\bar{p}_2). \end{aligned}$$

Furthermore, from (3.27), (A.2), and (A.3), we have

$$\begin{aligned} &\mathcal{A}_{21} = 3f_{300}p_1^2\bar{p}_1 + 3f_{030}p_2^2\bar{p}_2 + 3f_{120}(p_2^2\bar{p}_1 + 2p_1\bar{p}_2p_2) + 3f_{210}(\bar{p}_2p_1^2 + 2p_1p_2\bar{p}_1), \\ &\mathcal{A}_{12} = 3f_{300}\bar{p}_1^2p_1 + 3f_{030}\bar{p}_2^2p_2 + 3f_{120}(\bar{p}_2^2p_1 + 2\bar{p}_1p_2\bar{p}_2) + 3f_{210}(p_2\bar{p}_1^2 + 2\bar{p}_2p_1\bar{p}_1), \\ &\mathcal{A}_{30} = f_{300}p_1^3 + 3f_{120}p_1p_2^2 + 3f_{210}p_1^2p_2 + f_{030}p_2^3, \mathcal{A}_{03} = f_{300}\bar{p}_1^3 + 3f_{120}\bar{p}_1\bar{p}_2^2 + 3f_{210}\bar{p}_1^2\bar{p}_2 + 3f_{030}\bar{p}_2^3. \end{aligned}$$

Similarly, we have

$$F_2(\mathcal{P}\omega b_{n_H}(x)+z)=\sum_{r_1+r_2=2}\mathcal{A}_{r_1r_2}\omega_1^{r_1}\omega_2^{r_2}b_{n_H}^2(x)+S_2(\mathcal{P}\omega b_{n_H}(x),z)+O(|z|^2),$$

where

$$\begin{aligned}S_2(\mathcal{P}\omega b_{n_H}(x),z)=&2[f_{200}p_1z_1+f_{020}p_2z_2+f_{110}(p_2z_1+p_1z_2)]\omega_1 b_{n_H}(x)\\&+2[f_{200}\bar{p}_1z_1+f_{020}\bar{p}_2z_2+f_{110}(\bar{p}_2z_1+\bar{p}_1z_2)]\omega_2 b_{n_H}(x).\end{aligned}$$

Next, we will compute $h_{0,20}$, $h_{0,11}$, $h_{2n_H,20}$, and $h_{2n_H,11}$. It follows from [26]

$$M_2^2(h_n(\omega)b_n(x))=D_\omega(h_n(\omega)b_n(x))\mathfrak{D}\omega-\mathscr{L}(h_n(\omega)b_n(x))$$

that

$$\begin{pmatrix}\left[M_2^2(h_n(\omega)b_n(x)),\beta_{n_H}^{(1)}\right]\\ \left[M_2^2(h_n(\omega)b_n(x)),\beta_{n_H}^{(2)}\right]\\ \left[M_2^2(h_n(\omega)b_n(x)),\beta_{n_H}^{(3)}\right]\end{pmatrix}=2i\varpi_{n_H}[h_{n,20}\omega_1^2-h_{n,02}\omega_2^2]-\mathscr{L}_0(h_n(\omega)),$$

where

$$\mathscr{L}_0(h_n(\omega))=-(\frac{n}{l})^2\delta_0h_n(\omega)+L_0(h_n(\omega)).$$

By combining with (3.9) and (3.13), we obtain

$$f_2^2(\omega,0,0)=\tilde{F}_2\left(\mathcal{P}\omega b_{n_H}(x),0\right)-\mathcal{P}\left\langle Q\begin{pmatrix}\left[\tilde{F}_2\left(\mathcal{P}\omega b_{n_H}(x),0\right),\beta_{n_H}^{(1)}\right]\\ \left[\tilde{F}_2\left(\mathcal{P}\omega b_{n_H}(x),0\right),\beta_{n_H}^{(2)}\right]\\ \left[\tilde{F}_2\left(\mathcal{P}\omega b_{n_H}(x),0\right),\beta_{n_H}^{(3)}\right]\end{pmatrix}\right\rangle b_n(x).$$

Furthermore, by (3.28)–(3.31), we have

$$\begin{pmatrix}\left[f_2^2(\omega,0,0),\beta_{n_H}^{(1)}\right]\\ \left[f_2^2(\omega,0,0),\beta_{n_H}^{(2)}\right]\\ \left[f_2^2(\omega,0,0),\beta_{n_H}^{(3)}\right]\end{pmatrix}=\begin{cases}\frac{1}{\sqrt{l\pi}}\left(\mathcal{A}_{20}\omega_1^2+\mathcal{A}_{02}\omega_2^2+\mathcal{A}_{11}\omega_1\omega_2\right), & n=0,\\ \frac{1}{\sqrt{2l\pi}}\left(\tilde{\mathcal{A}}_{20}\omega_1^2+\tilde{\mathcal{A}}_{02}\omega_2^2+\tilde{\mathcal{A}}_{11}\omega_1\omega_2\right), & n=2n_H,\end{cases}$$

where $\tilde{\mathcal{A}}$ is given by

$$\begin{cases}\tilde{\mathcal{A}}_{i_1i_2}=\mathcal{A}_{i_1i_2}-2\left(\frac{n_H}{l}\right)^2\mathcal{A}_{i_1i_2}^d,\\ i_1,i_2=0,1,2,i_1+i_2=2,\end{cases}\tag{A.5}$$

where $\mathcal{A}_{i_1,i_2}^d$ is given by (3.31), and by matching the coefficients of $\omega_1^2$ and $\omega_1\omega_2$, we get

$$n=0,\begin{cases}\omega_1^2:2i\varpi_{n_H}h_{0,20}-L_0\left(h_{0,20}\right)=\frac{1}{\sqrt{l\pi}}\mathcal{A}_{20},\\ \omega_1\omega_2:-L_0\left(h_{0,11}\right)=\frac{1}{\sqrt{l\pi}}\mathcal{A}_{11},\end{cases}\tag{A.6}$$

and

$$n=2n_H,\begin{cases}\omega_1^2:2i\varpi_{n_H}h_{2n_H,20}-\mathscr{L}_0\left(h_{2n_H,20}\right)=\frac{1}{\sqrt{2l\pi}}\tilde{\mathcal{A}}_{20},\\ \omega_1\omega_2:-\mathscr{L}_0\left(h_{2n_H,11}\right)=\frac{1}{\sqrt{2l\pi}}\tilde{\mathcal{A}}_{11}.\end{cases}\tag{A.7}$$

Solving (A.6), we get

$$(2i\varpi_{n_H}E_3 - L_0)\, h_{0,20} = \frac{1}{\sqrt{l\pi}}\mathcal{A}_{20},$$

therefore,

$$h_{0,20} = (2i\varpi_{n_H}E_3 - L_0)^{-1}\frac{1}{\sqrt{l\pi}}\mathcal{A}_{20}.$$

Similarly, we obtain

$$h_{0,11} = (-L_0)^{-1}\frac{1}{\sqrt{l\pi}}\mathcal{A}_{11}.$$

Solving (A.7), we have

$$\mathscr{L}_0(h_n(\omega)) = -(\frac{n}{l})^2\delta_0 h_n(\omega) + L_0(h_n(\omega)).$$

We have

$$\left(2i\varpi_{n_H}E_3 + \frac{4n_H^2}{l^2}\delta_0 - L_0\right)h_{2n_H,20} = \frac{1}{\sqrt{2l\pi}}\tilde{\mathcal{A}}_{20},$$

therefore,

$$h_{2n_H,20} = \left(2i\varpi_{n_H}E_3 + \frac{4n_H^2}{l^2}\delta_0 - L_0\right)^{-1}\frac{\tilde{\mathcal{A}}_{20}}{\sqrt{2l\pi}},$$

where $\tilde{\mathcal{A}}_{20}$ is determined by (A.5). Similarly, we have

$$h_{2n_H,11} = \left(\frac{4n_H^2}{l^2}\delta_0 - L_0\right)^{-1}\frac{1}{\sqrt{2l\pi}}\tilde{\mathcal{A}}_{11}.$$